Journal of Medicinal Chemistry

Article

Rational Design of Small Peptides for Optimal Inhibition of Cyclooxygenase-2 (COX-2): Development of a Highly Effective Anti-inflammatory Agent

Palwinder Singh, Sukhmeet Kaur, Jagroop Kaur, Gurjit Singh, and Rajbir Bhatti

J. Med. Chem., **Just Accepted Manuscript** • DOI: 10.1021/acs.jmedchem.6b00134 • Publication Date (Web): 28 Mar 2016

ACS Publications

Journal of Medicinal Chemistry is published by the American Chemical Society. 1155 Sixteenth Street N.W., Washington, DC 20036

Rational Design of Small Peptides for Optimal Inhibition of Cyclooxygenase-2 (COX-2): Development of a Highly Effective Anti-inflammatory Agent

Palwinder Singh[a,*], Sukhmeet Kaur[a], Jagroop Kaur[a], Gurjit Singh[b], Rajbir Bhatti[b]

[a]UGC Sponsored Centre for Advanced Studies - Department of Chemistry, Guru Nanak Dev University, Amritsar- 143005, India

[b]Department of Pharmaceutical Sciences, Guru Nanak Dev University, Amritsar-143005, India

Abstract: Amongst the small peptides **2–31**; (H)Gly-Gly-Phe-Leu(OMe) (**30**) reduced prostaglandin production of COX-2, IC_{50} 60 nM vs 6000 nM for COX-1. The 5 mg Kg^{-1} dose of compound **30** rescued albino mice by 80% from capsaicin induced paw licking and recovered it by 60% from carageenan induced inflammation. The mode of action of compound **30** for targeting COX-2, iNOS and VGSC was investigated by using substance P, L-arginine and veratrine, respectively as the biomarkers. The interactions of **30** with COX-2 were supported by the isothermal calorimetry experiments showing K_a $6.10\pm1.10\times10^4$ mol^{-1} and ΔG -100.3 k J mol^{-1} in comparison to K_a 0.41×10^3 ±0.09 mol^{-1} and ΔG -19.2 ± 0.06 k J mol^{-1} for COX-1. Moreover, compound **30** did not show toxicity up to 2000 mg Kg^{-1} dose. Hence, we suggest peptide **30** as a highly potent and promising candidate for its further development into anti-inflammatory drug.

1. Introduction

Besides their key role as biocatalysts[1] and hormones,[2,3] small peptide/proteins are also identified with anti-cancer,[4,5] anti-diabetic,[6,7] anti-microbial[8] and anti-fungal[9] activities. The biological acceptability and the substrate specific properties of the proteins/enzymes have played a guiding role in the design of target specific small peptides and consequently, they have taken the centre-stage in the development of new drugs.[10-12] Given the major role of cyclooxygenase enzymes (housekeeping COX-1 and inducible COX-2) in regulating the arachidonic acid metabolic pathway[13-17] and the production of pro-inflammatory prostaglandins[18,19] by the inducible form of cyclooxygenase, COX-2 is the selective target of anti-inflammatory drugs. Starting with the use of aspirin, diclofenac, indomethacin as the non-steroidal anti-inflammatory drugs (NSAIDs),[20-22] the development of COXIBs[23-26] has provided some relief to the patients suffering from wide spectrum of inflammatory diseases. However, the cardiovascular side effects associated with the use of COXIBs is the limiting factor that has subdued the medicinal applications of this class of anti-inflammatory drugs[27-33] and hence still keeping the search for new chemical entities open. Various small peptides have been recently described as an alternative class of anti-inflammatory drugs.[34-36] But a major issue in the development of COX-2 inhibitors is to achieve optimal inhibition of the enzyme so that the side effect risks are kept at the possible minimum.

Based on our recent success in identifying the anti-inflammatory potential of indole appended peptides wherein the peptide component plays key role for the activity of the molecules[37] and also taking into consideration the detailed analysis of arachidonic acid (AA) bound COX-2 crystal coordinates;[38-40] here, we designed a series of small peptides. Specifically, the molecular modelling studies helped us in: (i) the design of such peptides which can occupy

the same place in the COX-2 active site which otherwise is inhabited by AA, (ii) incorporation of specific amino acids in the peptide so that the lipophilic – hydrophilic balance is maintained and (iii) providing information about the selectivity of the peptide for COX-2 over COX-1 (Table S1). The flexibility of the peptides to enter the COX-2 active site may help to selectively target the inflammatory tissues due to the higher concentration of the enzyme therein (more expression of COX-2) than the normal tissues (less concentration of the enzyme) and advantageously the side effects associated with COX-2 inhibitors may come down. Probably, the COX-2 concentration gradient in the inflammatory – non-inflammatory tissues has worked in our experiments (details will be given separately) for the identification of a highly promising anti-inflammatory agent. The synthesis of newly designed peptides was succeeded by their in-vitro and in-vivo COX-2 inhibition and anti-inflammatory properties.

2. Results and Discussion

The structural and volume similarity between the peptides and arachidonic acid (natural substrate of COX-2) strengthened the design of the new molecules. Given in the preferred primary structure, tri- and tetra- peptides were expected as the most suitable candidates for creating a competition with arachidonic acid for binding to the active site of the enzyme. Therefore, by selecting the proper amino acids (keeping in mind the optimal LogP of the molecule), the desired peptides were synthesized. The hydrophobic nature of the COX-2 active site made us to prefer the use of Gly, Ala, Val, Leu, Phe for making the peptide.

2.1. Chemistry

The desired peptides were procured by the coupling of N-Cbz protected amino acid with amino acid methyl ester hydrochloride by using ethyl chloroformate as the coupling reagent. For the synthesis of Gly–Ala–Val peptide; solution of triethylamine, ethylchloroformate and N-

CbzGly in THF was maintained at -10 ^{o}C. Addition of alanine methyl ester hydrochloride to the above solution and stirring the reaction mixture at 0 – 10 ^{o}C and then at room temperature (25 – 30 ^{o}C) for 12 h provided N-CbzGly–Ala(OMe) peptide. N-CbzGly–Ala(OMe) was hydrolyzed with 1N NaOH and the resulting N-CbzGly–Ala(OH) was further coupled with Val for procuring N-CbzGly–Ala–Val peptide. Treatment of this peptide with Pd-C/H_2 removed the Cbz group and finally Gly–Ala–Val peptide was isolated. Other peptides were synthesized through the same procedure (Table 1, Scheme S1-S5). All the synthesized compounds were characterized with NMR, mass and IR spectral techniques. The percentage purity was checked with qNMR (quantitative NMR) and optical purity was ascertained by using Chirobiotic® T 10 μm reverse phase chiral HPLC column. Reproducible ^{1}H NMR spectra of the compounds after 2/5 days ensured stability of the compounds in the solution ($CHCl_3$/DMSO) as well as in the solid form.

2.2. Biological studies

2.2.1. In-vitro COX-1, COX-2 inhibitory activity

All the peptides were subjected to enzyme immunoassays. For making the comparison, the dipeptides were also included in the enzyme inhibitory studies. Compounds were screened for COX-1 and COX-2 inhibition at four different molar concentrations (10^{-5} M – 10^{-8} M).[41] All the compounds were tested in triplicate and the average of three values with deviation <3% was taken for calculation. The enzyme inhibition assay is based on COX-1, COX-2 catalyzed production of prostaglandins during AA metabolism.

Enzyme inhibition = 1/conc of prostaglandin produced in each enzymatic reaction

The dipeptide **2** and **3** exhibited IC_{50} 1 μM and 2 μM, respectively for COX-2 whereas these two dipeptides did not affect COX-1 catalyzed reaction. Amongst compounds **6** – **9**, the COX-2

Table 1. Peptides synthesized for the present experiments and their IC_{50} (μM) against COX-1, COX-2.

Compd	Structure	% yield	IC_{50} (μM)[ψ]		Selectivity Index*
			COX-1	COX-2	
2	N-Cbz-Gly-Gly-OMe	55	>10	1	>10
3	N-Cbz-Gly-Gly-OH	50	>10	2	>10
6	N-Cbz-Gly-Ala-Val-OMe	50	8	0.1	80
7	N-Cbz-Gly-Ala-Val-OH	38	>10	3	>3
8	H_2N-Gly-Ala-Val-OMe	45	>10	10	>1
9	H_2N-Gly-Ala-Val-OH	45	9	0.2	45
10	N-Cbz-Gly-Ala-Val-Leu-OMe	25	>10	22	--
11	N-Cbz-Gly-Ala-Val-Leu-OH	17	>10	8	--
16	N-Cbz-Gly-Val-Ala-Leu-OMe	20	>10	19	--
17	N-Cbz-Gly-Val-Ala-Leu-OH	18	3	0.3	10
18	N-Cbz-Val-Gly-OMe	65	>10	75	--
19	N-Cbz-Val-Gly-OH	60	>10	55	--
20	N-Cbz-Val-Gly-Leu-OMe	45	>10	56	--
21	N-Cbz-Val-Gly-Leu-OH	40	>10	28	--
22	H_2N-Val-Gly-Leu-OMe	30	>10	10	--
23	H_2N-Val-Gly-Leu-OH	30	10	2	5
24	N-Cbz-Val-Gly-Leu-Ala-OMe	22	>10	0.08	>125
25	N-Cbz-Val-Gly-Leu-Ala-OH	22	0.3	0.05	6
28	N-Cbz-Gly-Gly-Phe-Leu-OMe	20	>10	20	--
29	N-Cbz-Gly-Gly-Phe-Leu-OH	18	3	0.5	6
30	H_2N-Gly-Gly-Phe-Leu-OMe	22	6	0.06	100

31	H_2N-Gly-Gly-Phe-Leu-OH	20	>10	0.4	>25
Diclofenac			0.07	0.02	3.5
Celecoxib			15	0.04	375

[Ψ]Average of the three values with deviation <3%. *IC_{50}(COX-1)/IC_{50}(COX-2)

inhibitory activity of compound **6** and **9** was appreciable, showing respective IC_{50} 0.1 and 0.2 μM. The selectivity index 80 for compound **6** was also significant whereas the selectivity of compound **9** for COX-2 over COX-1 was poor. Compounds **11**, **17** and **24** provided an excellent view of structure activity relationship. It was apparent that the difference in the sequence of amino acids in these three isomeric peptides was responsible for the difference in the activity of the compounds. Compound **24** with IC_{50} 0.08 μM for COX-2 displayed better enzyme inhibitory profile than that of compound **11** and **17.** After hydrolyzing the ester group of **24**, the IC_{50} of the resulting compound **25** for COX-2 was improved. Amongst the last category of compounds, **30** displayed higher efficacy for the inhibition of COX-2 enzyme with IC_{50} 0.06 μM and selectivity index 100 whereas its corresponding acid **31** exhibited poor inhibition of COX-2 (Table 1). Compound **29** showed considerable inhibition of catalytic activities of both COX-2 and COX-1, exhibiting negligible selectivity for COX-2 over COX-1. Amongst the other compounds tested here, compound **17** with IC_{50} 3 μM and 0.3 μM for COX-1 and COX-2, respectively exhibited poor selectivity for COX-2 over COX-1. IC_{50} of compounds **8**, **11** and **31** for COX-2 was 8 μM, 8 μM and 0.4 μM, respectively. Overall, the enzyme immunoassays identified compounds **24** and **30** with significant COX-2 inhibitory activity which was comparable to that of diclofenac and celecoxib. Desirably, the selectivity of compound **30** for COX-2 over COX-1 was higher than that of diclofenac and lower than the COX-2 selectivity of celecoxib.

The selectivity of compound **30** for COX-2 over COX-1 was also ascertained using human whole blood assay.[42,43] Concentration of TxB_2 (as a measure of TxA_2 formation and hence COX-1 activity) and PGE_2 (as a measure of COX-2 activity) was determined by ELISA. Compound **30** did not alter the formation of TxB_2 in comparison to the control whereas significant reduction in the PGE_2 formation was observed (Table 2). These results support the enzyme immunoassay for COX-2 selectivity of compound **30**.

Therefore, the trend of enzyme inhibitory activity of the peptides is parallel to the results of docking studies and explicitly justifies their design. Compound **6**, **24** and **30** were further screened for anti-inflammatory activity on mice and their physical interaction with COX-2 was also checked with the help of isothermal titration calorimetric (ITC) experiments.

Table 2. Inhibition of TxB_2 in calcium ionophore stimulated whole blood and PGE_2 in LPS stimulated whole blood by compound **30**

	TXB_2 ng/mL		PGE_2 ng/mL	
	-calcium Ionophore	+calcium Ionophore	-LPS	+LPS
control	1.5	8.5	2.2	15.5
Indomethacin (1 μM)		2.7		2.1
Compound **30** (1 μM)		5.8		0.08

2.2.2. In-vivo biological studies.

Swiss albino mice of either sex (25–35 g) were used in the present study. The animals were maintained at 22 ± 2 °C under 12 h light/12 h dark cycle with free supply of food and water. The study has been approved by the IAEC of Guru Nanak Dev University, Amritsar, Punjab, India.

2.2.2.1. Models for analgesic and anti-inflammatory activity. Capsaicin induced algesia as described in our previous studies was used.[44] Briefly, pain response was quantified as the number of paw lickings following capsaicin injection (1.6 µg in 20 µL) in the plantar surface of the hind paw. Formalin induced algesia was used to assess neurogenic and inflammatory phases of pain according to the method described by Hunskaar and Hole.[45] In brief, 20 µL of 2% formalin was injected into the plantar surface of the right hind paw of mouse after 30 min of treatment with standard/test compound and number of hind paw flinching were observed for first 5 min and at

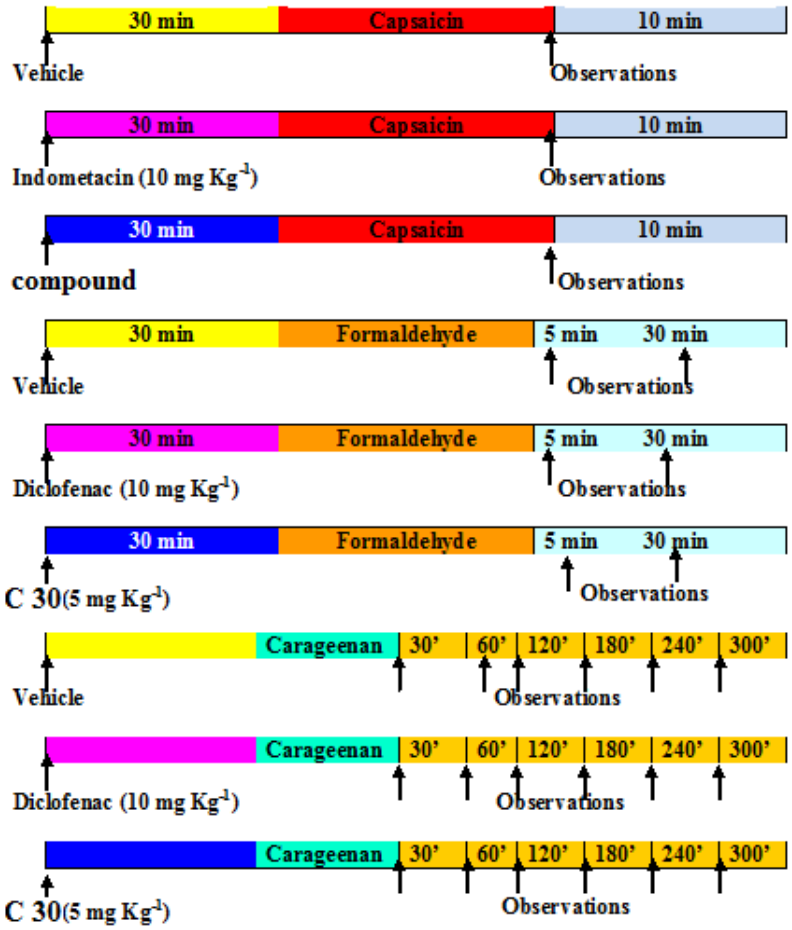

Figure 1. Schematic representation of experimental protocol for analgesic and anti-inflammatory studies.

30 min. The first phase indicates the neurogenic pain whereas the second phase indicates the inflammatory phase. To study the anti-inflammatory activity, carageenan induced paw edema model as previously described was used.[44] The schematic representation of the experimental protocol is given in figure 1.

For studying the involvement of cyclooxygenase and lipooxygenase pathway in the mode of action of the compound, the animals were pretreated with substance P. In order to check the involvement of nitric oxide pathway during the inhibition of algesia, the animals were pretreated with L-arginine and L-NAME (Figure 2). For investigating the involvement of voltage gated sodium channels (VGSC), calcium influx and potassium channels, the animals were pretreated with veratrine, A 23187 and glipizide, respectively (Figure 2).

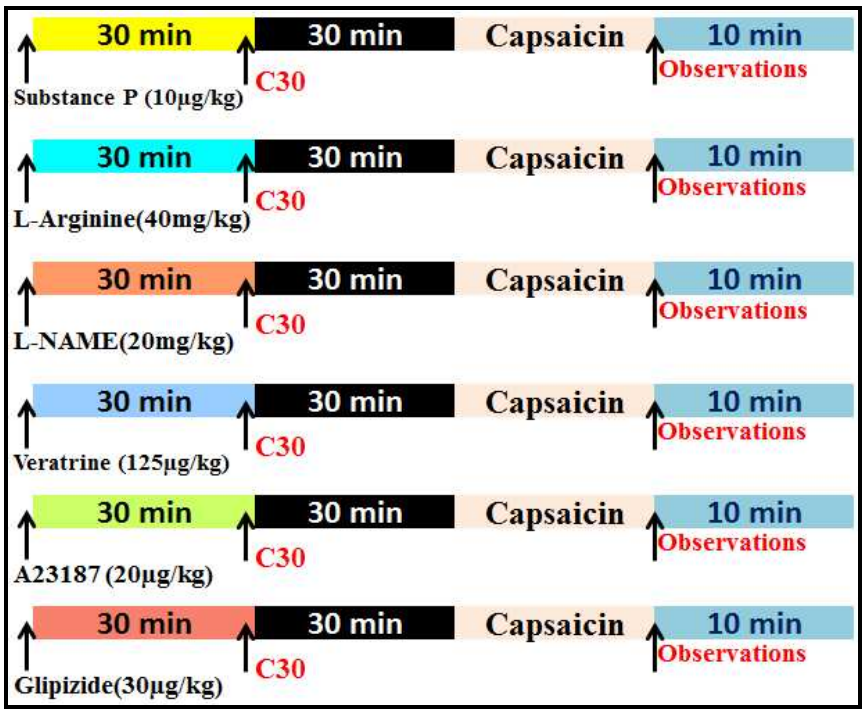

Figure 2. Schematic representation of experimental protocols for exploring the involvement of cyclooxygenase, lipooxygenase pathway (substance P), nitric oxide pathway (L-arginine, L-NAME), VGSC (veratrine), Calcium channel (A 23187) and potassium channels (Glipizide) in the observed analgesic effect of compound **30**.

2.2.2.2. Analgesic activity and anti-inflammatory activity. The treatment of animals with compound **30** (5 mg and 10 mg), compound **6** (5 mg and 10 mg) and compound **24** (5 mg and 10 mg) were found to produce a marked decrease in the number of paw lickings after capsaicin injection. Compound **30** was the most potent showing its effect comparable to the standard drug indomethacin (Figure 3) and it was subjected to further studies. It was observed that compound **30** treated mice produce a marked decrease in inflammation in carageenan induced paw edema and here the effect was similar to that of the standard drug diclofenac (Figure 4). In the formalin induced pain, the neurogenic phase (0-5 min) was not significantly decreased, whereas the inflammatory phase (15-30 min) of pain was attenuated by both the standard drug as well as compound **30** at a dose of 5 mg Kg^{-1} (Figure 5). Therefore, the animal based experiments substantiated the results of enzyme immunoassays and the potential of compound **30** as an anti-inflammatory drug.

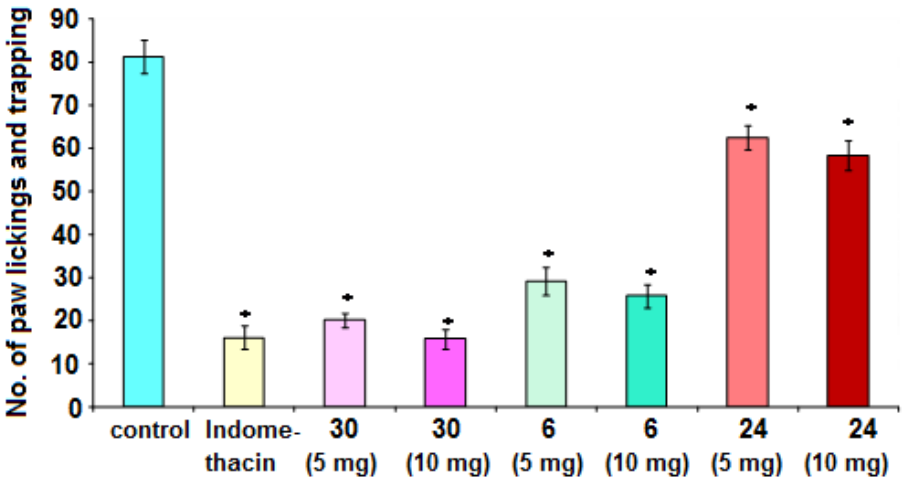

Figure 3. Effect of various compounds on capsaicin induced hyperalgesia. All values are expressed as mean ± SEM. * $p<0.05$ vs. control.

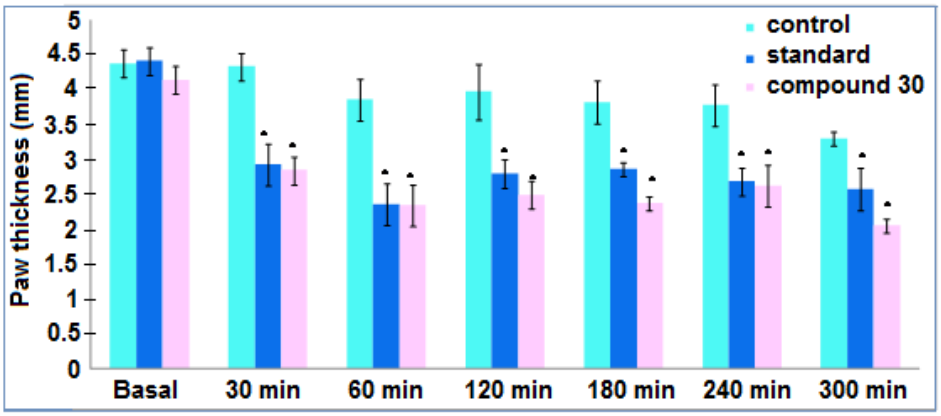

Figure 4. Effect of compound **30** on carageenan induced inflammation in mice. All values are expressed as mean ± SEM. * p<0.05 vs. control.

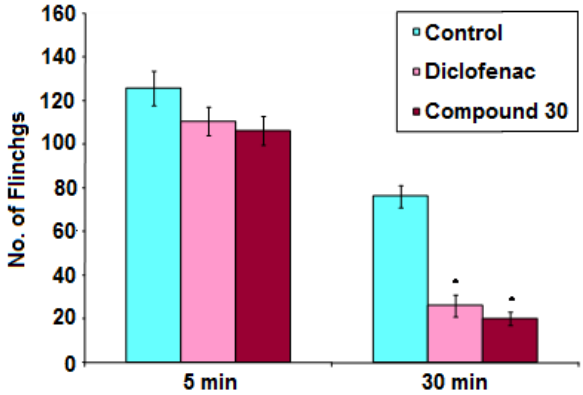

Figure 5. Effect of compound **30** on formalin induced hyperalgesia. All values are expressed as mean ± SEM. * p< 0.05 vs. formalin treated control.

2.2.2.3. Studies supporting the probable mode of action of the compounds. The excellent inhibition of COX-2 by compound **30** and its probable mode of action was checked by using substance P– a stimulator of COX-2, 5-LOX and promoter of prostaglandin/leukotriene production.[46,47] Pretreatment of the animal with substance P was found to reverse the analgesic effect of compound **30** (Figure 6) which indicated that COX-2 may be the probable target of **30** as it exhibited poor inhibition of 5-LOX (IC_{50} 6 μM). Nitric oxide formation by inducible nitric oxide synthase (iNOS) is well documented in pain mechanisms.[48] Therefore the modulation of

nitric oxide pathway was explored in the analgesic effect of compound **30**. Pretreatment with L-arginine, a nitric oxide precursor was found to reverse the analgesic effect of compound **30** whereas pretreatment with L-NAME, a nitric oxide synthase inhibitor did not alter the analgesic effect of compound **30** (Figure 6). These results indicate that a combination of modulation of COX-2 and nitric oxide formation might be involved in the analgesic effect of compound **30**. Remarkably, the pretreatment with A23187 (TxA2 stimulator) did not alter the analgesic effect of compound **30** and hence supporting the results of human whole blood assay, this compound does not affect COX-1.

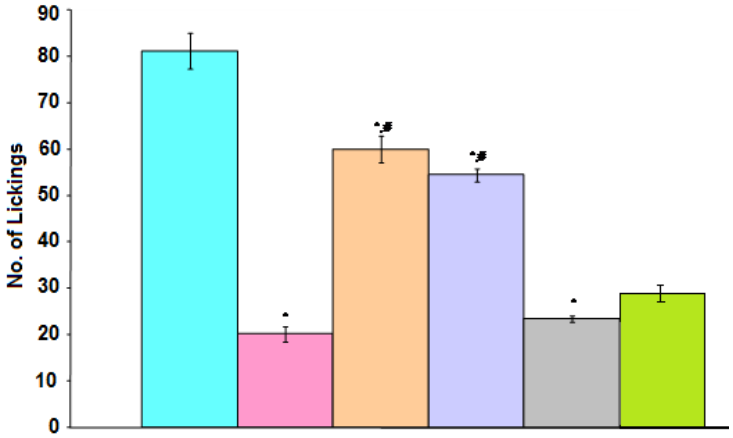

Capsaicin	+	+	+	+	+	+
Compound **30**	-	+	+	+	+	+
Substance P	-	-	+	-	-	-
L-Arginine	-	-	-	+	-	-
L-NAME	-	-	-	-	+	-
A-23187	-	-	-	-	-	+

Figure 6. Effect of Substance P, L-arginine and L-NAME on the analgesic effect of compound **30**. All values are expressed as mean ± SEM. * $p<0.05$ vs. control; # $p< 0.05$ vs. compound **30**.

In addition to the COX-2 and nitric oxide pathways, voltage gated sodium channels (VGSC) and increased calcium influx is also known to be involved in pain and inflammatory processes.[49,50] Furthermore, an increased influx of potassium culminating in hyperpolarization of free nerve endings is proposed to mediate analgesia.[51] Therefore, the involvement of these ion

channel pathways was investigated in the observed analgesic effect of compound **30**. Pretreatment with veratrine, a VGSC opener was found to ameliorate the analgesic effect of compound **30** partially although the reversal was not complete whereas pretreatment with glipizide, an ATP sensitive potassium channel (K_{ATP}) blocker, did not alter the analgesic effect of compound **30**. A comparison of the results of these experiments (Figure 6 and Figure 7) indicates that the inhibition of COX-2 is probably the major contributor to the analgesic effect of compound **30**.

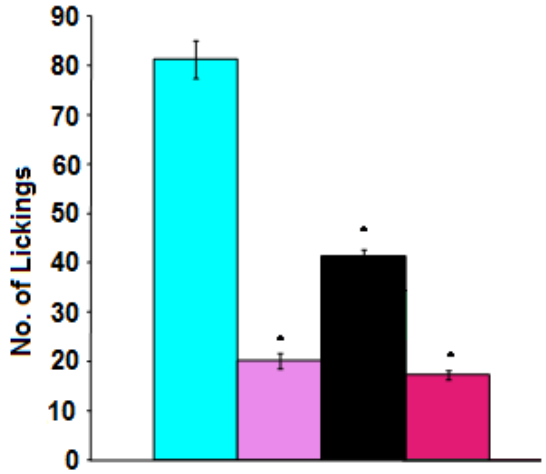

Capsaicin	+	+	+	+
Compound **30**	-	+	+	+
Veratrine	-	-	+	-
Glipizide	-	-	-	+

Figure 7. Modulation of VGSC, calcium and K_{ATP} channels in the analgesic effect of compound **30**. All values are expressed as mean ± SEM. * $p<0.05$ vs. control; # $p< 0.05$ vs. compound **30**.

2.2.2.4. Acute toxicity studies. OECD guidelines[52] (OECD, 2001) were followed for acute toxicity studies of compound **30**. Four groups of animals with three animals per group were taken. The first group was administered the vehicle and served as the control group; the second, third and the fourth groups were treated with compound **30** at doses of 50 mg Kg^{-1}, 300 mg Kg^{-1} and 2000 mg Kg^{-1} respectively. All the treatments were administered after 4 h of fasting.

Thereafter, the animals were observed continuously for the first four hours and periodically for 24 h. After 14 days, one animal each in control and highest dose (2000 mg Kg^{-1}) was sacrificed and histological studies were conducted by using H and E staining. No gross behavioral abnormality was observed in any of the four groups of animals. No significant changes were evident in the myocardium or liver of the animals treated with the highest dose of compound **30** (2000 mg Kg^{-1}) as compared to the control group (Figure 8).

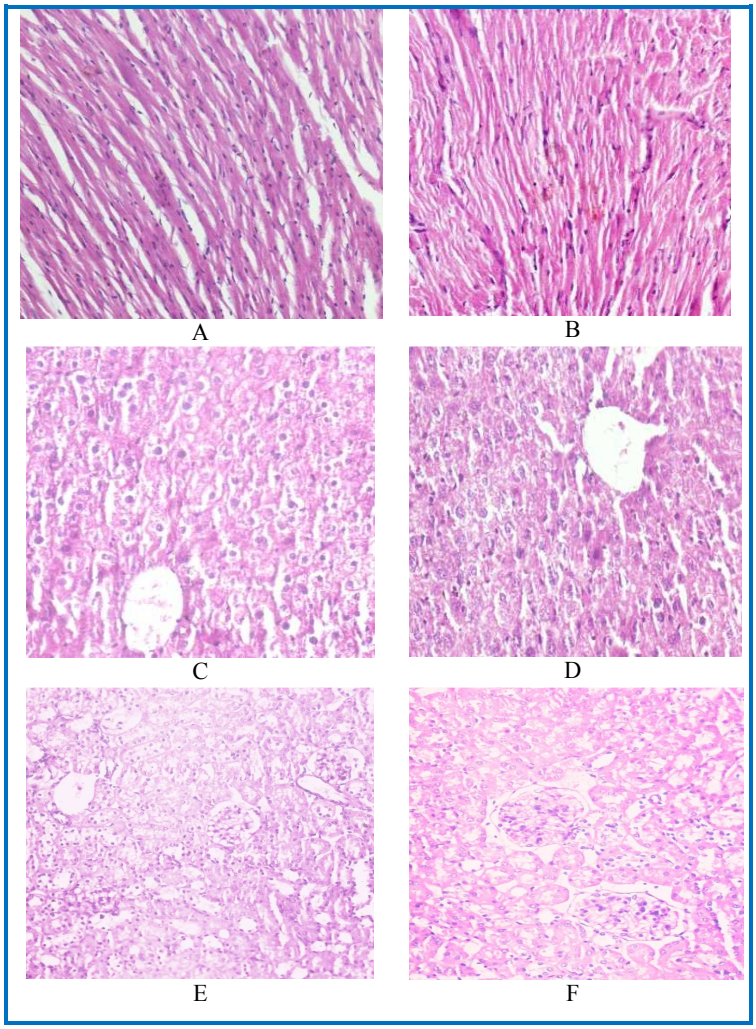

Figure 8. Histology myocardium of control (A, 20x) and compound **30** treated (B, 20x); liver of control (C, 20x) and compound **30** treated (D, 20x); kidneys of control (E, 20x) and compound **30** treated (F, 20x).

2.2.3. Isothermal calorimetric (ITC) experiments

ITC is one of the most precise techniques to measure the affinity between the macromolecule and the small molecule. Since ITC measures heat released or absorbed during binding, it is the only technique which allows simultaneous determination of all binding parameters viz. the binding constant (K), enthalpy (ΔH) and entropy (ΔS) in a single experiment. The solution of peptide **30** (in the syringe) was injected into the enzyme solution in HEPES buffer (pH 7.4) taken in the sample cell. In one experiment, 19 consecutive injections of 2 μL of 100 μM compound were given to the sample cell after regular time intervals of 120 s so that equilibrium is ensured in each titration point. Upon each titration, the amount of heat released or absorbed was measured and used to determine the association constant (K_a), binding enthalpy (ΔH) and entropy (ΔS). The total heat Q produced/absorbed in the active cell, determined at fractional saturation Θ after the ith injection, is given by equation 1

$$Q = n\,\Theta M_t\,\Delta H V_o \qquad (1)$$

where M_t is the total concentration of the enzyme, V_0 is the cell volume, n is the total number of binding sites in the enzyme, and ΔH is the molar heat of ligand binding.

The enthalpy change for the ith injection ΔH(i) for an injection volume dVi is defined by equation 2

$$\Delta H(i) = Q(i) + dV_i/V_o\,[Q(i)-Q(i-1)/2] - Q(i-1) \qquad (2)$$

The various parameters determined from ITC experiment and the binding isotherm for the titration of compound **30** against COX-2 and COX-1 are given in Table 2.

Table 2. Isothermal calorimetric data and binding isotherm of compound **30** for COX-2 and COX-1.

	Physical parameters obtained from ITC data*	
	COX-2	COX-1
K_a (M^{-1})	(6.10±1.10)x10^4	(0.41±0.09) x 10^3
ΔH (kJ/mol)	-107.0±1	-99.2±1
TΔS (kJ/mol)	-6.7±0.03	-80.0±1
ΔG (kJ/mol)	-100.3±1	-19.20±0.06

*average of the three experiments

Binding isotherm for COX-1 **Binding isotherm for COX-2**

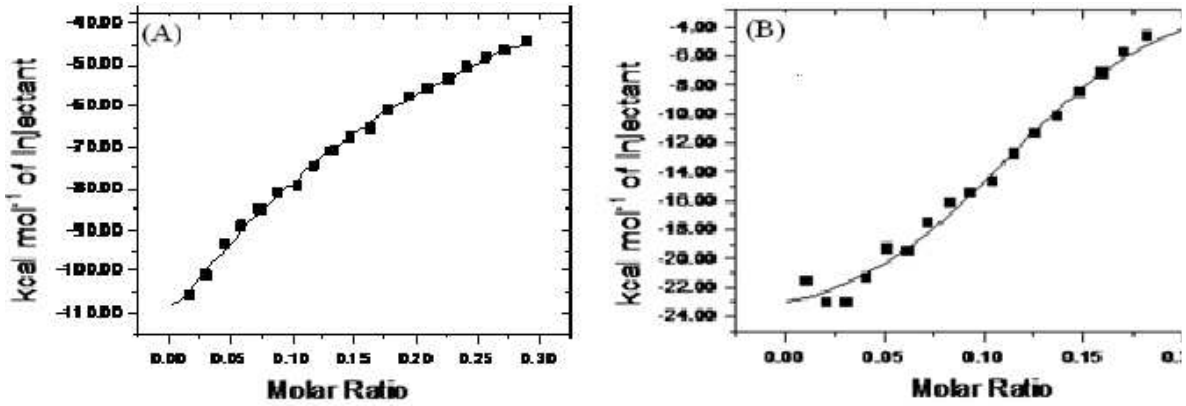

2.2.4. Molecular docking studies

In order to support the experimental results and to have an insight into the nature of interactions between the test compounds and the active site amino acid residues of the enzyme, molecular docking studies were carried out. Crystal co-ordinates of COX-2 (PDB ID 1CVU)[53] were downloaded from the protein data bank (www.rcsb.org). The molecular docking was performed using Schrodinger (Schrödinger Release 2014-4: Maestro, version 10.0, Schrödinger, LLC, New York, NY, 2014)[54-58] software package. Docking of arachidonic acid in the active site of COX-2 and root mean square deviation (RMSD) 1.18 Å to the X-ray structure validated the

docking procedure (Figure S81, supporting information). The most active compound **30**, identified in the present investigations, showed H-bond interactions through its carbonyl group with Y355 (1.89 Å) and R120 (1.68 Å, 2.20 Å). Hence, the two most crucial amino acids of COX-2 catalytic site (Y355 and R120)[59-63] were captured by compound **30**. The NH_2 group of compound **30** was also H-bonded to Y115 (2.14 Å) and S119 (2.17 Å) (Figure 9). It was apparent from the comparison between the docking pose of compound **30** and AA that the hydrophobic part of compound **30** (benzyl and iso-butyl groups) occupies the same place where AA was present (as seen in the COX-2 crystal coordinates with AA, 1CVU) (Figure 10). Additionally, the polar part of compound **30** constituted by two amide groups and one amino group extends into the polar sub-pocket of the active site (Figure S85). The positioning of compound **30** in the interacting pocket of COX-2 is clearly visible in figure 11.

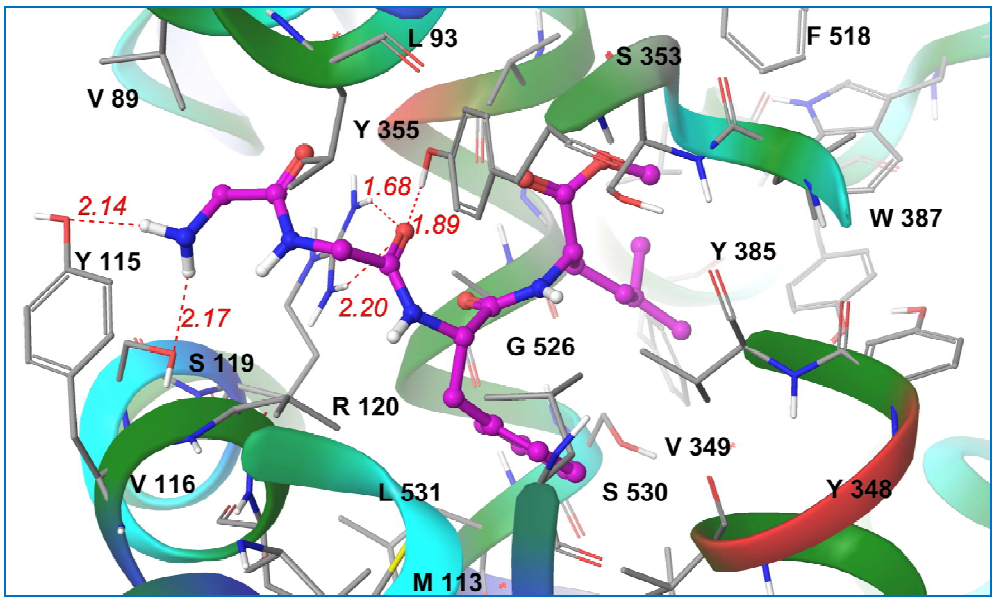

Figure 9. Compound **30** docked in active site of COX-2 (PDB ID 1CVU). Red lines represent H-bond with bond length in Å.

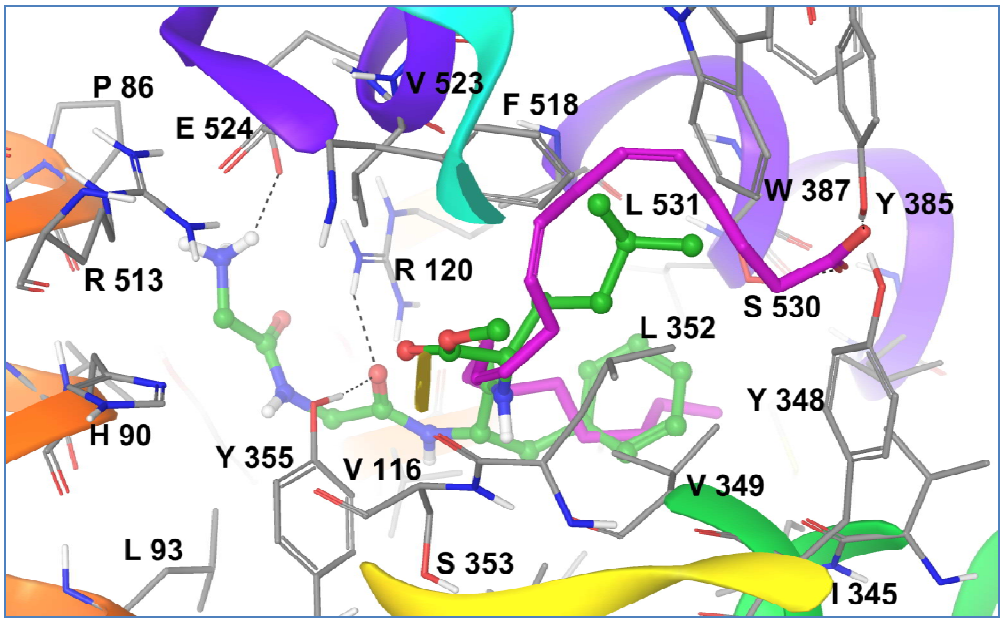

Figure 10. Compound **30** (green**)** and arachidonic acid (purple) in the active site of COX-2 (pdb ID 1CVU).

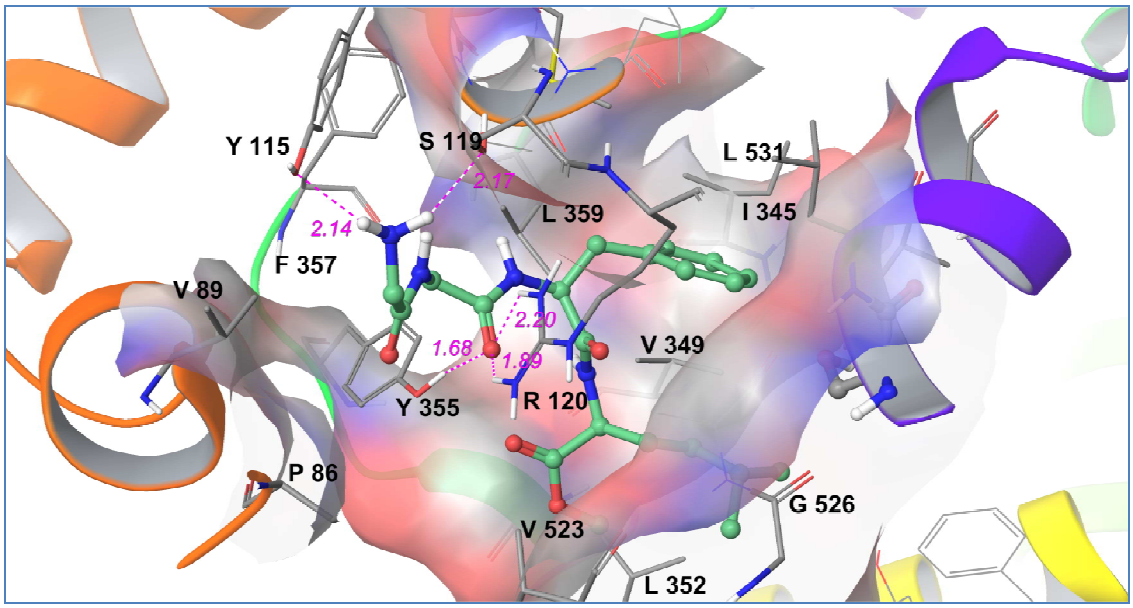

Figure 11. N-Cbz-Gly-Gly-Phe-Leu-OMe (**30**) was positioned in the interacting pocket of 1CVU with hydrogen bonds (dotted lines in Magenta).

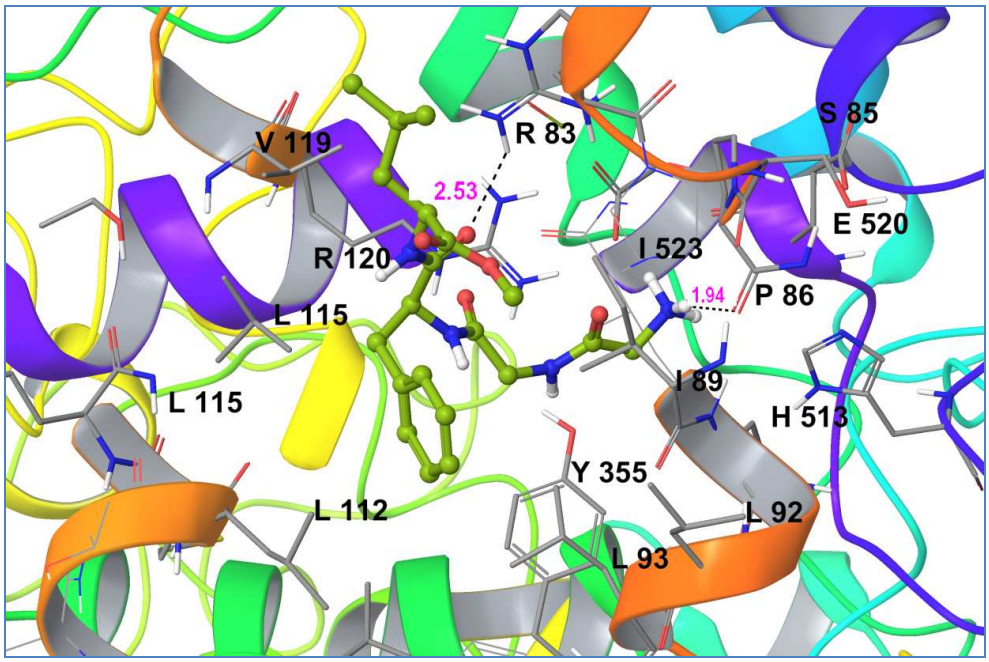

Figure 12. N-Cbz-Gly-Gly-Phe-Leu-OMe (**30**) (green) docked in the active site of COX-1 (PDB ID 1EQG).

Further to support the selectivity of compound **30** for COX-2 over COX-1, as observed during the enzyme immunoassays, compound **30** was also docked in the active site of COX-1. As it is apparent from figure 12, compound **30** entered into the active site of COX-1 but in contrast to its contacts in the active site of COX-2, it does not interact with Y355 and R120. However, the H-bond interactions of compound **30** with R83 and P86 were visible. Moreover, the docking score of compound **30** for COX-2 and COX-1 was quite different whereas expectedly, arachidonic acid exhibited similar docking score for COX-2 and COX-1 (Table S1). Evidently, a nice correlation between the experimental results and the results of molecular docking studies was observed.

For getting more support to the docking results of compound **30**, the molecular docking of compound **6** in the active site of COX-2 and COX-1 was also investigated. Compound **6** showed H-bond interactions of 1.94 Å, 2.44 Å and 2.44 Å between its carbonyl group and Y355, R120

residues of COX-2 active site (Figure 13) whereas no such type of interactions were visible when it was docked in the active site of COX-1 (Figure S84).

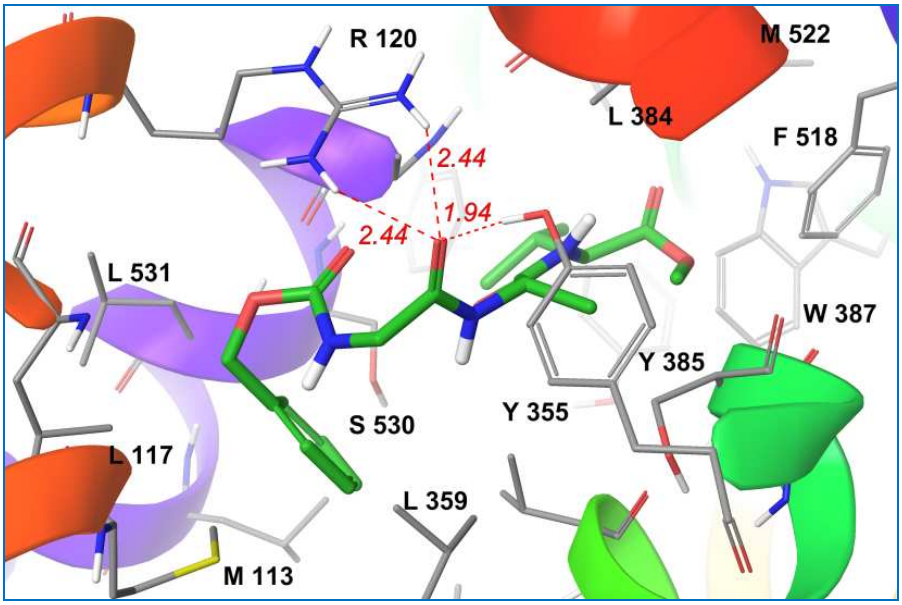

Figure 13. Compound **6** (green) docked in active site of COX-2 (PDB ID 1CVU). Red lines represent H-Bond with bond length in Å.

Since compound **30** was found to inhibit the NOS pathway also, its interaction in the active site of iNOS was checked through molecular docking. NOS is present in three different isoforms- neuronal NOS or nNOS (Type I or NOS-1), inducible NOS or iNOS (Type II or NOS-2) and endothelial NOS or eNOS (Type III or NOS-3). In contrast to nNOS and eNOS, which are constitutively active, expression of iNOS is induced by cytokines and pathogens. Docking of the peptides in the active site of iNOS was performed. Crystal co-ordinates of iNOS (PDB ID 3E7G)[64] were downloaded from the protein data bank (www.rcsb.org). Compound **30** showed interactions with the active site residues though its docking score (-5.97 Kcal/mol) was less than that for COX-2. Compound **30** showed H-bond interactions through its carbonyl group with amino group of Q263 (2.10 Å) and hydroxyl group of Y347 (2.14 Å). It displayed three H-bond interactions with propionate group of heme of iNOS protein (Figure 14, Figure 15).

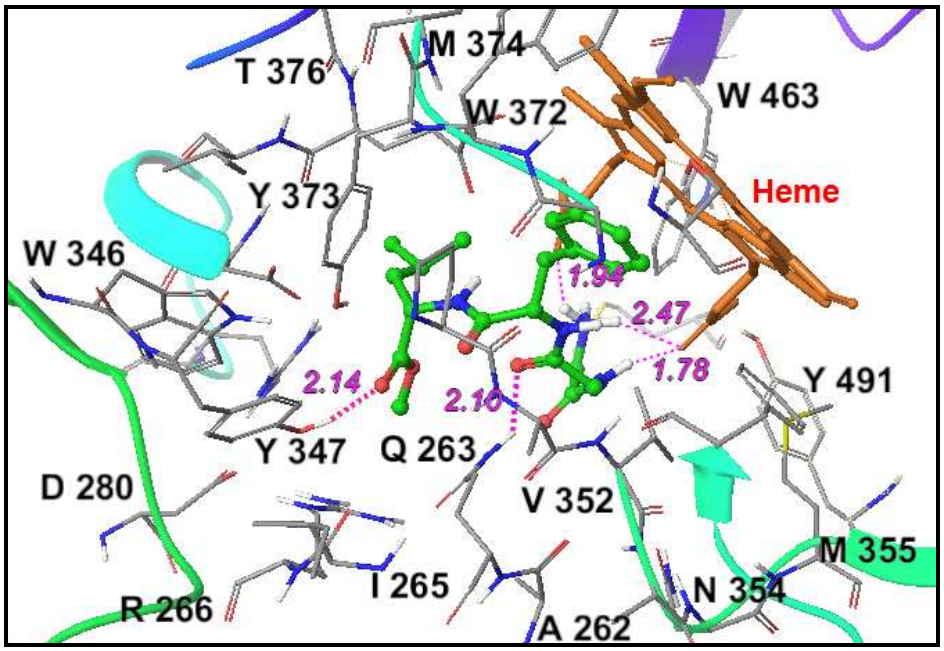

Figure 14. N-Cbz-Gly-Gly-Phe-Leu-OMe (**30**, green) docked in the active site of iNOS (PDB ID 3E7G). Magenta lines represent H-Bond with bond length in Å.

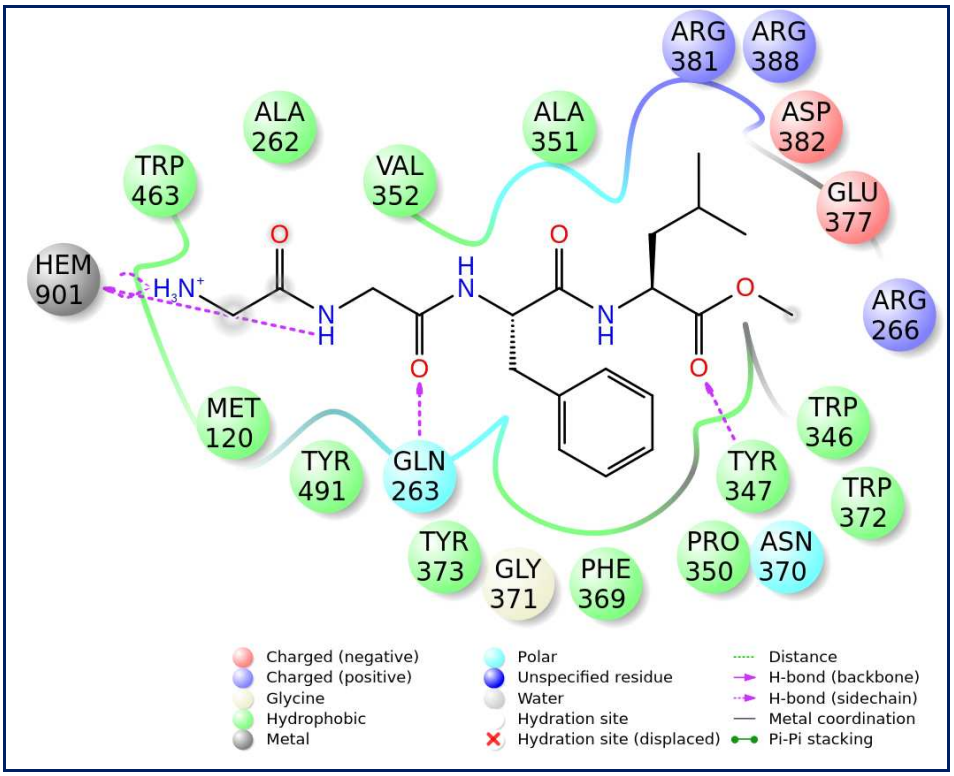

Figure 15. 2D diagram of binding pose of compound **30** in the active site of iNOS.

2.2.5. 3D-QSAR (Quantitative Structure Activity Relationship Studies) model

Being a new class of COX-2 inhibitors and showing appreciable results, it was interesting to perform QSAR studies with the series of peptides under present investigation. By using PLS with three factors, the Gaussian-based QSAR model was generated by correlating with five fields: steric, electrostatic, hydrophobic, HBD, and HBA (Figure 16, Figure S88). An R^2CV value of 0.68 were derived from the LOO cross-validation method and non-cross-validation analysis yielded an R^2 value of 0.96 with a standard error of estimate of 0.21 and an F ratio of 96.3 (Table 3, Table S3). The contributions of the steric, electrostatic, hydrophobic, HBD, and HBA fields were 0.39, 0.08, 0.27, 0.21 and 0.03, respectively. The field contributions of steric (0.39) and hydrophobic (0.27) intensities were higher when compared to the electrostatic, HBA, and HBD which indicate their significant role in the protein–ligand interactions. Figure 16a explains steric contours map with green region on the ligand molecules represent favorable effect of bulky substituents and grey region shows negative effect of bulky substituents and substitution in this region may reduce the activity. The positive effect of bulky substituent was clearly observed in the case of tetrapeptide **30**. Replacement of alanine residues of tetrapeptide **16** with phenyl alanine (bulky substituent) resulted in higher activity of tetrapeptide **30**. Similar effect was observed in case of tetrapeptide **24** where the bulky leucine residue was present in the green region.

Figure 16b illustrates electrostatic contours map. Blue contours in the molecule represent that electropositive groups may increase the activity while red regions represent that electronegative group may enhance the activity. The electrostatic contribution to the activity is 0.08 which is quite less. In Figure 16c, white contour in the hydrophobic plot indicates that hydrophobic groups at those regions are disfavored. A yellow contour indicates that hydrophobic groups are

tolerated at that position. The yellow contour closer to the leucine residue in compound **11**, **17** and **24** resulted in better activity. The effect of hydrophobicity on the activity of the compound was quite evident from the difference in the LogP of compound **30** and **31** and the corresponding change in their IC_{50} for COX-2 (Table S2). Figure 16d shows the HBA contour maps. The red contour in the HBA indicates that HBA groups lead to the improved activity whereas magenta contour indicates that presence of HBA groups lead to reduced activity. In general, in all the molecules the carbonyl group of amide bond is very much responsible for establishing hydrogen bonds with the Arg 120 and Y355 (these two amino acids of COX-2 are required for the inhibition of NSAID's). Figure 16e shows the HBD contours where areas favored by donors are shown in blue violet, and unfavorable areas are shown in cyan color. The contribution of HBD is negligible (0.03). The QSAR model also showed significant fitness of observed activity with the predicted activity for the training and test set of compounds (Table S3) (Figure 17). A common pharmacophores model was generated by the alignment of all ligands (active and inactive) to the pharmacophore (Figure 18).

Table 3: PLS statistical parameters of the selected 3D-QSAR model

PLS Factors	SD	R^2	R^2 CV	R^2 Scramble	Stability	F	P	RMSE	Q^2	Pearson -R
1	0.8715	0.6291	0.2862	0.4916	0.576	34.2	0.0256	1.19	0.8610	0.2917
2	0.4211	0.8193	0.4638	0.7289	0.432	52.3	3.91-007	0.98	0.5211	0.2210
3	0.2116	0.9602	0.6811	0.8436	0.694	96.3	1.21e-008	0.73	0.7532	0.5102

SD, standard deviation of the regression; R, squared value of R^2 for the regression; F, variance ratio. Large value of F indicate a more statistically regression; P, significance level of variance ratio. Smaller value indicate a greater degree of confidence; RMSE, root mean square error; Q, squared value of Q^2 for the predicted activities; Pearson-R, Pearson-R value for the correlation between the predicted and observed activity for the test set.

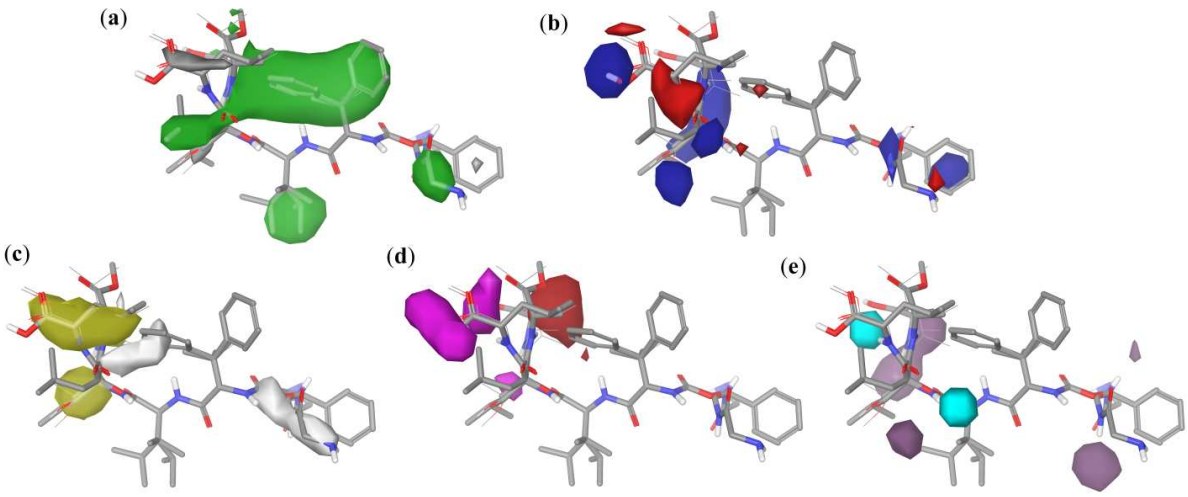

Figure 16. QSAR visualization of various subsituents effects: (a) steric contour map (grey, negative saturation and green is positive saturation); (b) Electrosatatic contour map (blue positive saturation and red negative saturation; (c) Hydrophobic contour map (white, negative saturation and yellow positive saturation), (d) H-Bond contour map (magenta negative saturation and maroon positive saturation); (e) H-Bond Donor contour map (cyan represents negative saturation and purple is positive saturation). Active molecules are shown in tube and inactive molecules in wire.

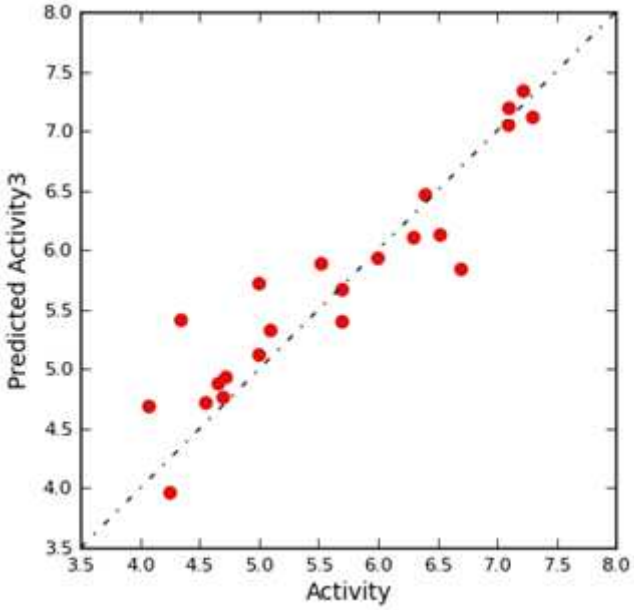

Figure 17. Fitness graph between observed activity versus predicted activity for training and test set compounds.

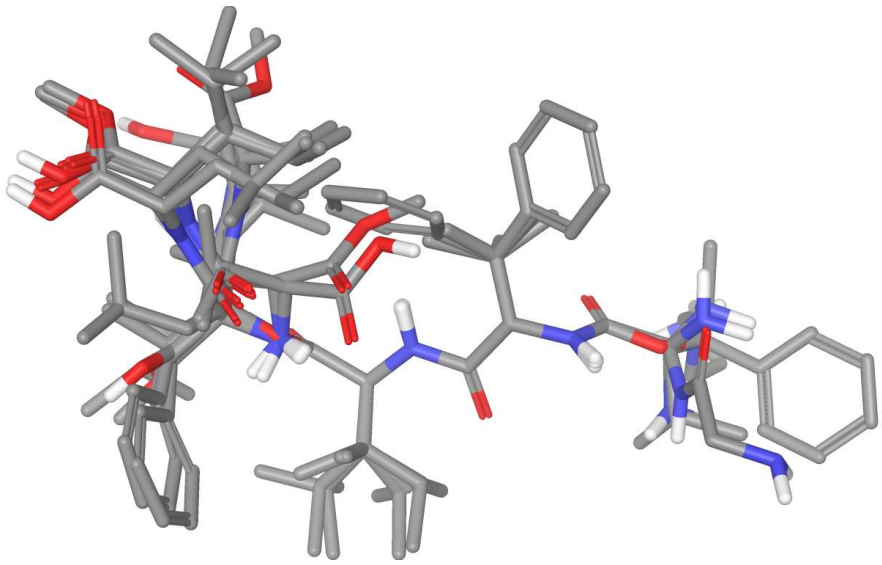

Figure 18. Common pharmacophore generation (peptide backbone): alignment of all ligands (active and inactive) to the pharmacophore.

3. Conclusions

We have identified tetrapeptide **30** which exhibited inhibition of COX-2 with IC_{50} 60 nM and appreciable selectivity over COX-1. Testing of this compound on albino mice showed reversal of algesia and inflammation with as much efficacy but better selectivity for COX-2 as shown by the standard drug indomethacin and diclofenac. The mechanistic studies indicated that compound **30** was acting through the inhibition of COX-2 channel of arachidonic acid pathway and inhibition of inducible nitric oxide synthase whereas inhibition of VGSC and calcium influx was not significant. Appreciable binding constant of compound **30** with COX-2, calculated from the ITC data, and its considerable interactions in the active site of COX-2 and iNOS, as depicted from the molecular modeling studies, supported the in-vitro and in-vivo biological results. Overall, we came out with a peptide based lead molecule for anti-inflammatory drug.

4. Experimental

4.1. General

Melting points were determined in capillaries and are uncorrected. ^{1}H and ^{13}C NMR spectra were recorded on Bruker 500 MHz and 125 MHz NMR spectrometer, respectively using $CDCl_3$ and/or DMSO-d_6 as solvent. Chemical shifts are given in ppm with TMS as an internal reference. *J* values are given in Hertz. Signals are abbreviated as singlet, s; doublet, d; double-doublet, dd; triplet, t; multiplet, m. Mass spectra were recorded on Bruker micrOTOF Q II Mass spectrometer. The purity of compound was determined using qHNMR method (Absolute qHNMR with Internal Calibration).[65] The purity of >95% of the target analyte was determined using the following equation:

$[P\%] = n_{IC} \cdot Int_t \cdot MW_t \cdot m_{IC} / n_t \cdot Int_{IC} \cdot MW_{IC} \cdot m_S * P_{IC}$

MW = molecular weights

P = purity of internal calibrant

m_{IC} = amount of internal calibrant, m_s = amount of sample (compound)

Int = integral, n = no of protons giving rise to a given NMR signal

IC = internal calibrant, t = target analyte or compound

General Procedure for peptide synthesis

Procedure A. L-AA (amino acid) (0.01 mol) was dissolved in 10 ml (0.01 mol) of 4M sodium hydroxide solution, cooled to 0 ^{o}C and 0.01 mol of benzyl chloroformate and 0.01 mol of 4M sodium hydroxide solution was added alternatively and portion wise with shaking and cooling during 30 min. The mixture was allowed to stir for another 1 h. Then the reaction mixture was extracted with 2x15 ml portions of ether and aqueous part was acidified with dil HCl. The liberated oil was extracted with ether and dried over anhydrous sodium sulphate. The ether was evaporated to obtain the desired NCbz-AA (90%).

Procedure B. N-Cbz-AA (1 mmol) was dissolved in the THF (50 ml). After cooling the solution to -10 ^{o}C, triethylamine (0.021 mol) was added followed by the addition of ethylchloroformate (0.014 mol). The mixture was stirred at -10 ^{o}C for 15 min. A cooled solution of the neutralized AA methyl ester hydrochloride (1.2 mmol) in 5 ml THF was added to the reaction mixture. The reaction mixture was stirred for 1 h at 0 ^{o}C to -10 ^{o}C at and then at room temperature for 12 h. After completion of the reaction (TLC), 5% Na_2CO_3 solution was added to the reaction mixture and extracted with ethyl acetate. The organic layer was dried over anhydrous Na_2SO_4 and evaporated under vacuum and purified through column chromatography using ethyl acetate-hexane as eluent to get pure N-Cbz-AA-AA methyl ester (70%). Acidification of aqueous part with 10% HCl gave unreacted N-Cbz-AA. Treatment of N-Cbz-AA–AA methyl ester with 1N NaOH in acetone-water (3:2) followed by acidification of the reaction mixture and extraction with ethyl acetate provided pure N-Cbz-AA–AA dipeptide.

Procedure C. To a solution of N-Cbz-AA-AA in MeOH, 10% Pd/C (0.1%) was added. H_2 gas was passed through reaction mixture for 3-4 h. The completion of reaction mixture was monitored by TLC. After completion of reaction, the catalyst was removed by filtration and the filtrate was concentrated in vacuum to obtain the desired peptide.

4.1.1. N-Cbz-Glycine

N-Cbz-Gly was synthesized according to general procedure A as white solid, yield 95%, mp 117 ^{o}C (lit mp 120 ^{o}C).

4.1.2. N-Cbz Gly-Gly-OMe (2)

Compound **2** was synthesized according to general procedure B as white solid; yield 55%, mp 65 ^{o}C; ^{1}H NMR (500 MHz, $CDCl_3$) δ 3.76 (s, 3H, OCH_3), 3.93 (d, J = 5.0 Hz, 2H, CH_2), 4.05 (d, J = 5.0 Hz, 2H, CH_2), 5.14 (s, 2H, CH_2), 5.58 (t, J=5.1 Hz, 1H, NH_{Gly1}), 6.69 (br, 1H, NH_{Gly2}),

7.32 – 7.37 (m, 5H, ArH), ^{13}C NMR (125 MHz, normal/DEPT-135) δ 41.1 (-ve, CH_2), 44.4 (-ve, CH_2), 52.4 (+ve, OCH_3), 67.3 (-ve, CH_2), 128.1 (+ve, ArCH), 128.2 (+ve, ArCH), 128.5 (+ve, ArCH), 136.0 (ab, ArC), 156.6 (C=O), 169.3 (C=O), 170.1 (C=O); HRMS (microTOF-QII, MS, ESI): Calcd for $C_{13}H_{16}N_2O_5$ ($[M+Na]^+$) 303.0951, found 303.0959.

4.1.3. N-Cbz Gly-Gly-OH (3)

Compound **3** was synthesized according to general procedure B as white solid; yield 50%, mp 110 ^oC; ^{1}H NMR (500 MHz, DMSO-d_6) δ3.66 (d, J = 6.2 Hz, 2H, CH_2), 3.77 (d, J = 5.8 Hz, 2H, CH_2), 5.04 (s, 2H, CH_2),7.33 – 7.48 (m, 5H, ArH), 7.49 (t, J = 5.9 Hz, 1H, NH_{Gly1}), 8.15 (t, J = 5.3 Hz, 1H, NH_{Gly2}),12.58 (br, 1H, OH); ^{13}C NMR (125 MHz, normal/DEPT-135) δ 41.0 (CH_2), 43.8 (CH_2), 65.9 (CH_2), 128.1 (+ve, ArCH), 128.2 (+ve, ArCH), 128.8 (+ve, ArCH), 137.4 (ab, ArC), 156.9 (C=O), 169.9 (C=O), 171.6 (C=O); HRMS (microTOF-QII, MS, ESI): Calcd for $C_{12}H_{14}N_2O_5$ ($[M+H]^+$) 267.0978 found 267.0975.

4.1.4. N-Cbz Gly-Ala-Val-OMe (6)

Compound **6** was synthesized according to general procedure B as white solid; yield 50%, mp 108 ^oC; $[\alpha]_D^{25}$= -50° (C=1, $CHCl_3$); ^{1}H NMR (500 MHz, $CDCl_3$, 25 ^oC, TMS): δ 0.87-0.90 (m, 6H, 2xCH_3), 1.35 (d, J = 6. 4 Hz, 3H, CH_3), 2.12-2.16 (m, 1H, CH), 3.71 (s, 3H, OCH_3), 3.90 (br, 2H, CH_2),4.48-4.50 (m, 1H, CH_{Val}), 4.65-4.68 (m, 1H, CH_{Ala}), 5.10 (s, 2H, CH_2), 5.80 (d, J= 2.60 Hz, 1H, NH_{Gly}), 7.05 (br, 2H, NH_{Val}+NH_{Ala}) 7.26-7.34 (m, 5H, ArH); ^{13}C NMR (125 MHz, normal/DEPT-135) δ 17.7 (+ve, CH_3), 18.4 (+ve, CH_3), 18.9 (+ve, CH_3), 31.1 (+ve, CH), 44.3 (-ve, CH_2), 48.8 (+ve, CH), 52.1 (+ve, OCH_3), 57.3 (+ve, CH), 67.1 (-ve, CH_2), 128.1 (+ve, ArCH), 128.2 (+ve, ArCH), 128.3 (+ve, ArCH), 128.7 (+ve, ArCH), 128.8 (+ve, ArCH), 136.2 (ab, ArC), 156.6 (C=O), 168.9 (C=O), 172.1 (C=O), 172.2 (C=O); HRMS (microTOF-QII, MS, ESI): Calcd for $C_{19}H_{27}N_3O_6$ ($[M+Na]^+$) 416.1792, found 416.1817.

4.1.5. N-Cbz Gly-Ala-Val-OH (7)

Compound **7** was synthesized according to general procedure B as white solid; yield 38%, mp 160 ^{o}C, $[\alpha]_D^{25}$= -50° (C=1, MeOH); ^{1}H NMR (500 MHz, DMSO-d_6, 25 ^{o}C, TMS): δ 0.88 (d, J = 6.6 Hz, 6H, 2xCH_3), 1.20 (d, J=6.6 Hz, 3H, CH_3), 2.04-2.08 (m, 1H, CH), 3.58-3.68 (m, 2H, CH_2),4.11-4.14 (m, 1H, CH_{Ala}), 4.42-4.46 (m, 1H, CH_{Val}), 5.03 (s, 2H, CH_2), 7.31-7.38 (m, 5H; ArH), 7.45 (t, J = 6.5 Hz, 1H, NH_{Gly}), 7.95-7.98 (m, 2H, NH_{Ala}+NH_{Val}), 12.58 (br, 1H, OH); ^{13}C NMR (125 MHz, normal/DEPT-135) δ 18.4 (+ve, CH_3), 18.7 (+ve, CH_3), 19.5 (+ve, CH_3), 30.2 (+ve, CH), 43.8 (-ve, CH_2), 48.2 (+ve, CH), 57.6 (+ve, CH), 65.9 (-ve, CH_2), 128.1 (+ve, ArCH), 128.2 (+ve, ArCH), 128.8 (+ve, ArCH), 137.5 (ab, ArC), 156.9 (C=O), 169.0 (C=O), 172.8 (C=O), 173.2 (C=O); IR ($CHCl_3$): ν= 3329 (OH), 2966, 2927 (NH), 1712 (C=O), 1651 (C=O), 1219 (C-N) cm^{-1}; HRMS (microTOF-QII, MS, ESI): Calcd for $C_{18}H_{25}N_3O_6$ ([M+Na]$^+$) 402.1635, found 402.1626.

4.1.6. NH_2 Gly-Ala-Val-OMe (8)

Compound **8** was synthesized according to general procedure B and C as a semi- solid; yield 45%; $[\alpha]_D^{25}$= -30° (C=1, MeOH); ^{1}H NMR (500 MHz, DMSO-d_6, 25 ^{o}C, TMS): δ 0.86-0.89 (m, 6H, 2xCH_3), 1.20 (d, J = 6.5 Hz, 3H, CH_3), 2.02-2.06 (m, 1H, CH), 3.13 (br, 2H, CH_2), 3.63 (s, 3H, OCH_3), 4.14-4.17 (m, 1H, CH_{Val}), 4.45 (br, 1H, CH_{Ala}), 8.09 (br, 2H, NH_2), 8.22-8.23 (br, 2H, NH_{Val}+NH_{Ala}); ^{13}C NMR (125 MHz, normal/DEPT-135) δ 18.6 (+ve, CH_3), 19.2 (+ve, CH_3), 19.3 (+ve, CH_3), 30.2 (+ve, CH), 44.5 (-ve, CH_2), 47.8 (+ve, CH), 52.1 (+ve, OCH_3), 57.9 (+ve, CH), 172.2 (C=O), 172.3 (C=O), 173.0 (C=O); HRMS (microTOF-QII, MS, ESI): Calcd for $C_{11}H_{21}N_3O_4$ ([M+H]$^+$) 260.1614, found 260.1605.

4.1.7. NH_2 Gly-Ala-Val-OH (9)

Compound **9** was synthesized according to general procedure B and C as white solid; 45% yield, mp 85 ^{o}C, $[\alpha]_D^{25}$= -40° (C=1, MeOH); ^{1}H NMR (500 MHz, DMSO-d_6, 25 ^{o}C, TMS): δ 0.88 (d, J = 2.1 Hz, 3H, CH_3), 0.89 (d, J = 2.0 Hz, 3H, CH_3), 1.23 (d, J=7.0 Hz, 3H, CH_3), 2.03-2.08 (m, 1H, CH), 3.55-3.58 (m, 2H, CH_2),4.12-4.15 (m, 1H, CH_{Val}), 4.49-4.55 (m, 1H, CH_{Ala}), 7.96 (t, J = 5.2 Hz, 2H, NH_2), 8.13 (d, J=9.0 Hz, 1H, NH_{Val}), 8.51 (d, J=7.6 Hz, 1H, NH_{Ala}); ^{13}C NMR (125 MHz, normal/DEPT-135) δ 18.2 (+ve, CH_3), 18.9 (+ve, CH_3), 19.4 (+ve, CH_3), 30.1 (+ve, CH), 40.5 (-ve, CH_2), 48.4 (+ve, CH), 57.6 (+ve, CH), 165.7 (C=O), 172.5 (C=O), 173.2 (C=O); HRMS (microTOF-QII, MS, ESI): Calcd for $C_{10}H_{19}N_3O_4$ ([M+Na]$^+$) 268.1267, found 268.1268.

4.1.8. NCbz-Gly-Ala-Val-Leu-OMe (10)

Compound **10** was synthesized according to general procedure B and C as white solid, yield 25%, mp 155 ^{o}C, ^{1}H NMR (500 MHz, DMSO-d_6, 25 ^{o}C, TMS): δ 0.88-0.92 (m, 12H, 4xCH_3), 1.38 (d, J = 6.8 Hz, 3H, CH_3), 1.51-1.65 (m, 3H, CH+CH_2), 2.01-2.02 (m, 1H, CH), 3.61 (s, 3H, OCH_3), 4.09-4.14 (m, 2H, CH_2), 4.50-4.92 (m, 3H, CH_{Ala}+CH_{Val}+CH_{Leu}), 5.12 (s, 2H, CH_2), 7.30-7.35 (m, 5H, ArH), 7.47 (t, J= 5.6 Hz, 1H, NH_{Gly}), 7.99 (d, J = 8.1 Hz, 1H, NH_{Val}), 8.01 (d, J = 7.6 Hz, 1H, NH_{Ala}), 8.07 (br, 1H, NH_{Leu}); ^{13}C NMR (125 MHz, normal/DEPT-135) 18.4 (+ve, CH_3), 18.8 (+ve, CH_3),19.5 (+ve, CH_3), 22.4 (+ve, CH_3), 22.6 (+ve, CH_3), 24.1 (+ve, CH), 30.2 (+ve, CH), 39.5 (-ve, CH_2), 43.8 (-ve, CH_2), 48.2 (+ve, CH), 50.9 (+ve, CH), 53.1 (OCH_3), 57.6 (+ve, CH), 65.8 (-ve, CH_2), 128.0 (+ve, ArCH), 128.2 (+ve, ArCH), 128.7 (+ve, ArCH), 137.5 (ab, ArC), 156.9 (C=O), 169.0 (C=O), 170.6 (C=O), 172.8 (C=O), 173.1 (C=O).HRMS (microTOF-QII, MS, ESI): Calcd for $C_{25}H_{38}N_4O_7$ ([M+Na]$^+$) 507.2823, found 507.3005.

4.1.9. N-Cbz Gly-Ala-Val-Leu-OH (11)

Compound **11** was synthesized according to general procedure B as white solid; yield 17%, $[\alpha]_D^{25}$= -30° (C=1, MeOH), mp 115 ^{o}C; ^{1}H NMR (500 MHz, DMSO-d_6, 25 ^{o}C, TMS): δ 0.82-

0.89 (m, 12H, 4xCH_3), 1.16 (d, *J*= 7.4 Hz, 3H, CH_3), 1.48-1.63 (m, 3H, CH+CH_2), 1.96-2.00 (m, 1H, CH), 3.61-3.66 (m, 2H, CH_2), 4.15-4.29 (m, 2H, CH_{Ala}+CH_{Val}), 4.37-4.43 (m, 1H, CH_{Leu}), 5.03 (s, 2H, CH_2), 7.31-7.35 (m, 5H, ArH), 7.44 (t, *J*= 6.45 Hz, 1H, NH_{Gly}), 7.81 (d, *J*= 9.0 Hz, 1H, NH_{Val}), 7.96 (d, *J* = 7.7 Hz, 1H, NH_{Ala}), 8.06 (d, *J*=7.5 Hz, 1H, NH_{Leu}), 12.48 (br, 1H, OH); ^{13}C NMR (125 MHz, normal/DEPT-135) 18.2 (+ve, CH_3), 18.5 (+ve, CH_3), 19.7 (+ve, CH_3), 21.9 (+ve, CH_3), 23.5 (+ve, CH_3), 24.8 (+ve, CH), 31.5 (+ve, CH), 40.6 (-ve, CH_2), 44.0 (-ve, CH_2), 48.5 (+ve, CH), 50.7 (+ve, CH), 57.7 (+ve, CH), 66.0 (-ve, CH_2), 128.3 (+ve, ArCH), 128.4 (+ve, ArCH), 128.9 (+ve, ArCH), 137.7 (ab, ArC), 157.1 (C=O), 169.5 (C=O), 171.0 (C=O), 172.7 (C=O), 174.6 (C=O).HRMS (microTOF-QII, MS, ESI): Calcd for $C_{24}H_{36}N_4O_7$ ($[M+Na]^+$) 515.2476, found 515.2497.

4.1.10. N-Cbz-Gly-Val-Ala-Leu-OMe (16)

Compound **16** was synthesized according to the general procedure B as white solid, yield 20%, mp 170 ^{o}C, $[\alpha]_D^{25}$ = -60° (C=1, $CHCl_3$); ^{1}H NMR (500 MHz, DMSO-d_6, 25 ^{o}C, TMS): δ 0.79-0.89 (m, 12H, 4xCH_3), 1.20 (d, *J*= 7.0 Hz, 3H, CH_3), 1.48-1.55 (m, 3H, CH+CH_2), 1.91-1.94 (m, 1H, CH), 3.61 (s, 3H, OCH_3), 3.66 (d, *J* = 6.1 Hz, 2H, CH_2), 4.22-4.32 (m, 3H, CH_{Ala}+CH_{Val}+CH_{Leu}), 5.03 (s, 2H, CH_2), 7.31-7.37 (m, 5H, ArH), 7.45 (t, *J*= 5.5 Hz, 1H, NH_{Gly}), 7.74 (d, *J*= 8.5 Hz, 1H, NH_{Val}), 8.10 (d, *J* = 7.2 Hz, 1H, NH_{Ala}), 8.14 (d, *J* = 7.5 Hz, 1H, NH_{Leu}); ^{13}C NMR (125 MHz, normal/DEPT-135) 18.3 (+ve, CH_3), 18.3 (+ve, CH_3),19.5 (+ve, CH_3), 21.7 (+ve, CH_3), 23.2 (+ve, CH_3), 24.5 (+ve, CH), 31.3 (+ve, CH), 40.2 (-ve, CH_2), 43.2 (-ve, CH_2), 48.2 (+ve, CH), 50.6 (+ve, CH), 52.2 (OCH_3), 57.5 (+ve, CH), 65.8 (-ve, CH_2), 128.1 (+ve, ArCH), 128.2 (+ve, ArCH), 128.8 (+ve, ArCH), 137.5 (ab, ArC), 156.9 (C=O), 169.3 (C=O), 170.8 (C=O), 172.7 (C=O), 173.3 (C=O).HRMS (microTOF-QII, MS, ESI): Calcd for $C_{25}H_{38}N_4O_7$ ($[M+H]^+$) 507.2813, found 507.2852.

4.1.11. N-Cbz Gly-Val-Ala-Leu-OH (17)

Compound **17** was synthesized according to general procedure B as white solid; yield 18%, mp115 ^{o}C, $[\alpha]_D^{25}$ = -50° (C=1, MeOH); ^{1}H NMR (500 MHz, DMSO-d_6, 25 ^{o}C, TMS): δ 0.79-0.89 (m, 12H, 4XCH_3), 1.20 (d, *J*= 7.0 Hz, 3H, CH_3), 1.49-1.53 (m, 2H, CH+ 1H of CH_2), 1.61-1.69 (m, 1H, 1H of CH_2), 1.92-1.94 (m, 1H, CH), 3.66 (s, 3H, OCH_3), 3.66 (d, J=7.0 Hz, 2H, CH_2), 4.21-4.23 (m, 2H, CH_{Ala}+CH_{Va}), 4.30-4.33 (m, 1H, CH_{Leu}), 5.03 (s, 2H, CH_2), 7.30-7.36 (m, 5H, ArH), 7.45 (t, *J*= 7.2 Hz, 1H, NH_{Gly}), 7.74 (d, *J*= 8.5 Hz, 1H, NH_{Val}), 7.99 (d, *J* = 8.2 Hz, 1H, NH_{Leu}), 8.11 (d, *J* = 7.8 Hz, 1H, NH_{Ala}), 12.49 (br, 1H, OH); ^{13}C NMR (125 MHz, normal/DEPT-135) 17.9 (+ve, CH_3), 18.3 (+ve, CH_3), 19.5 (+ve, CH_3), 21.7 (+ve, CH_3), 23.3 (+ve, CH_3), 24.6 (+ve, CH), 31.3 (+ve, CH), 40.4 (-ve, CH_2), 43.8 (-ve, CH_2), 48.3 (+ve, CH), 50.5 (+ve, CH), 57.5 (+ve, CH), 65.8 (-ve, CH_2), 128.1 (+ve, ArCH), 128.2 (+ve, ArCH), 128.8 (+ve, ArCH), 137.5 (ab, ArC), 156.9 (C=O), 169.3 (C=O), 170.8 (C=O), 172.4 (C=O), 174.3 (C=O).HRMS (microTOF-QII, MS, ESI): Calcd for $C_{24}H_{36}N_4O_7$ ($[M+Na]^+$) 515.2476, found 515.2485.

4.1.12. N-Cbz-Valine

N-Cbz Valine was synthesized according to general procedure A.

4.1.13. N-Cbz-Val-Gly-OMe (18)

Compound **18** was synthesized according to general procedure B as white solid, yield 65 %, mp 80 ^{o}C; $[\alpha]_D^{25}$ = -30° (C=1, $CHCl_3$); ^{1}H NMR (500 MHz, $CDCl_3$, 25 ^{o}C, TMS) δ 0.94 (d, *J* = 6.8 Hz, 3H, CH_3), 0.98 (d, *J* = 6.8 Hz, 3H, CH_3), 2.15-2.17 (m, 1H, CH),3.75 (s, 3H, OCH_3), 4.08-3.99 (m, 3H, CH+CH_2), 5.11–5.05 (m, 2H, CH_2), 5.45 (d, *J* = 8.2 Hz, 1H, NH_{Val}), 6.63 (br, 1H, NH_{Gly}), 7.37 – 7.26 (m, 5H, ArH); ^{13}C NMR (125 MHz, $CDCl_3$) δ 17.7 (+ve, CH_3), 19.1 (+ve, CH_3), 31.0 (+ve, CH), 41.1 (-ve, CH_2), 52.3 (+ve, OCH_3), 60.3 (+ve, CH), 67.1 (-ve, CH_2),

128.0 (+ve, ArCH), 128.2 (+ve, ArCH), 128.5 (+ve, ArCH), 136.1 (ab, ArC), 156.4 (C=O), 170.1 (C=O), 171.6 (C=O); HRMS (microTOF-QII, MS, ESI): Calcd for $C_{16}H_{22}N_2O_5$ ($[M+H]^+$) 323.1601, found 323.1631.

4.1.14. N-Cbz-Val-Gly-OH (19)

Compound **19** was synthesized according to general procedure B as an oil, yield 60 %; $[\alpha]_D^{25}$ = -20° (C=1, $CHCl_3$); ^{1}H NMR (500 MHz, $CDCl_3$, 25 ^{o}C, TMS) δ 0.93 (d, *J* = 6.7 Hz, 3H, CH_3), 0.96 (d, *J* = 6.7 Hz, 3H, CH_3), 2.05-2.09 (m, 1H, CH), 4.03 (br, 2H, CH_2), 4.17-4.20 (m, 1H, CH), 5.04–5.13 (m, 2H, CH_2), 5.92 (d, *J* = 9.2 Hz, 1H, NH_{Val}), 7.21 (t, *J* = 5.0 Hz, 1H, NH_{Gly}), 7.32 – 7.35 (m, 5H, ArH); ^{13}C NMR (125 MHz, $CDCl_3$) δ 17.9 (+ve, CH_3), 19.1 (+ve, CH_3), 31.1 (+ve, CH), 41.2 (-ve, CH_2), 60.2 (+ve, CH), 67.2 (-ve, CH_2), 127.9 (+ve, ArCH), 128.2 (+ve, ArCH), 128.5 (+ve, ArCH), 136.0 (ab, ArC), 156.9 (C=O), 172.4 (C=O), 172.5(C=O); HRMS (microTOF-QII, MS, ESI): Calcd for $C_{15}H_{20}N_2O_5$ ($[M+H]^+$) 309.1444, found 309.1412.

4.1.15. N-Cbz-Val-Gly-Leu-OMe (20)

Compound **20** was synthesized according to general procedure B as white solid, yield 45%, mp 75 ^{o}C; $[\alpha]_D^{25}$ = - 40° (C=1, $CHCl_3$); ^{1}H NMR (500 MHz, $CDCl_3$, 25 ^{o}C, TMS): δ 0.90-0.96 (m, 12H, 4xCH_3), 1.53-1.65 (m, 3H, CH+CH_2), 2.09-2.13 (m, 1H, CH), 3.68 (s, 3H, OCH_3), 3.90-3.93 (m, 1H, CH), 4.03-4.09 (m, 2H, CH_2), 4.57-4.60 (m, 1H, CH), 5.02-5.13 (m, 2H, CH_2), 5.60-5.68 (m, 1H, NH_{Val}), 7.08-7.13 (m, 1H, NH_{Leu}), 7.21 (br, 1H, NH_{Gly}), 7.31-7.34 (m, 5H, ArH); ^{13}C NMR (125 MHz, normal/DEPT-135) δ 17.9 (+ve, CH_3), 19.2 (+ve, CH_3), 21.8 (+ve, CH_3), 22.7 (+ve, CH_3), 24.7 (+ve, CH_3), 30.9 (+ve, CH), 41.1 (CH_2), 43.0 (-ve, CH_2), 50.8 (+ve, CH), 52.2 (+ve, OCH_3), 60.6 (+ve, CH_3), 67.0 (-ve, CH_2), 128.0 (+ve, ArCH), 128.1 (+ve, ArCH), 128.5 (+ve, ArCH), 136.0 (ab, ArC), 156.5 (C=O), 168.7 (C=O), 172.1 (C=O), 173.3

(C=O); HRMS (microTOF-QII, MS, ESI): Calcd for $C_{22}H_{33}N_3O_6$ ([M+Na]$^+$) 458.2261, found 458.2286.

4.1.16. N-Cbz-Val-Gly-Leu-OH (21)

Compound **21** was synthesized according to general procedure B as oily (40%); $[\alpha]_D^{25}$= -40° (C=1, $CHCl_3$); ^{1}H NMR (500 MHz, $CDCl_3$, 25 ^{o}C, TMS): δ 0.84-0.88 (m, 12H, 4xCH_3), 1.49-1.65 (m, 3H, CH+CH_2), 1.95-1.99 (m, 1H, CH), 3.73-3.74 (m, 2H, CH_2), 3.84-3.87 (m, 1H, CH), 3.97-3.98 (m, 1H, CH), 4.99-5.07 (m, 2H, CH_2), 7.31 (d, *J* = 5.2 Hz, 1H, NH_{Val}), 7.36-7.37 (m, 5H, ArH), 7.94 (d, *J* = 8.1 Hz, 1H, NH_{Leu}), 8.20 (t, *J* = 5.6 Hz, 1H, NH_{Gly}), 12.59, (br, 1H, OH); ^{13}C NMR (125 MHz, normal/DEPT-135) δ 18.6 (+ve, CH_3), 19.6 (+ve, CH_3), 21.8 (+ve, CH_3), 23.1 (+ve, CH_3), 24.5 (+ve, CH_3), 30.4 (+ve, CH), 40.4 (CH_2), 42.0 (-ve, CH_2), 50.6 (+ve, CH), 60.8 (+ve, CH_3), 65.9 (-ve, CH_2), 128.1 (+ve, ArCH), 128.2 (+ve, ArCH), 128.8 (+ve, ArCH), 137.4 (ab, ArC), 156.7 (C=O), 169.2 (C=O), 171.9 (C=O), 173.2 (C=O); HRMS (microTOF-QII, MS, ESI): Calcd for $C_{21}H_{31}N_3O_6$ ([M+H]$^+$) 422.2285, found 422.2348.

4.1.17. H_2N-Val-Gly-Leu-OMe (22)

Compound **22** was synthesized according to general procedure B and C as white solid, yield 30%, mp 75 ^{o}C; $[\alpha]_D^{25}$ = - 40° (C=1, $CHCl_3$); ^{1}H NMR (500 MHz, DMSO-d_6, 25 ^{o}C, TMS): δ 0.83-0.89 (m, 12H, 4xCH_3), 1.48-1.61 (m, 3H, CH+CH_2), 1.89-1.93 (m, 1H, CH), 3.62 (s, 3H, OCH_3), 3.77 (d, *J* = 4.8 Hz, 2H, CH_2), 3.97-3.98 (m, 1H, CH), 4.28-4.31 (m, 1H, CH), 8.24 (d, *J* = 7.5 Hz, 1H, NH_{Val}), 8.27 (br, 1H, NH_{Gly}), 8.52 (d, *J* = 7.5 Hz, 1H, NH_{Leu}); ^{13}C NMR (125 MHz, normal/DEPT-135) δ 17.4 (+ve, CH_3), 19.0 (+ve, CH_3), 21.8 (+ve, CH_3), 23.1 (+ve, CH_3), 24.6 (+ve, CH_3), 31.6 (+ve, CH), 40.0 (-ve, CH_2), 41.9 (-ve, CH_2), 50.6 (+ve, CH), 53.3 (+ve, OCH_3), 60.2 (+ve, CH_3), 166.5 (C=O), 169.4 (C=O), 173.3 (C=O); HRMS (microTOF-QII, MS, ESI): Calcd for $C_{14}H_{27}N_3O_4$ ([M+Na]$^+$) 324.1893, found 324.1970.

4.1.18. H_2N-Val-Gly-Leu-OH (23)

Compound **23** was synthesized according to general procedure B and C as semi-Solid, yield 30%, ^{1}H NMR (500 MHz, DMSO-d_6, 25 ^{o}C, TMS): δ 0.83-0.89 (m, 12H, 4xCH_3), 1.48-1.61 (m, 3H, CH+CH_2), 1.89-1.93 (m, 1H, CH), 3.62 (s, 3H, OCH_3), 3.77 (d, J = 4.8 Hz, 2H, CH_2), 3.97-3.98 (m, 1H, CH), 4.28-4.31 (m, 1H, CH), 8.24 (d, J = 7.5 Hz, 1H, NH_{Val}), 8.27 (br, 1H, NH_{Gly}), 8.52 (d, J = 7.5 Hz, 1H, NH_{Leu}); ^{13}C NMR (125 MHz, normal/DEPT-135) δ 18.2 (+ve, CH_3), 19.2 (+ve, CH_3), 21.4 (+ve, CH_3), 22.7 (+ve, CH_3), 24.2 (+ve, CH_3), 30.1 (+ve, CH), 40.0 (-ve, CH_2), 41.7 (-ve, CH_2), 50.2 (+ve, CH), 50.4 (+ve, CH_3), 168.9 (C=O), 171.6 (C=O), 172.9 (C=O); HRMS (microTOF-QII, MS, ESI): Calcd for $C_{13}H_{25}N_3O_4$ ($[M+H]^+$) 288.1917, found 288.1988.

4.1.19. N-Cbz Val-Gly-Leu-Ala-OMe (24)

Compound **24** was synthesized according to general procedure B as white solid; yield 22%, mp 145 ^{o}C, $[\alpha]_D^{25}$ = -40° (C=1, $CHCl_3$); ^{1}H NMR (500 MHz, $CDCl_3$, 25 ^{o}C, TMS): δ 0.87-0.95 (m, 12H, 4xCH_3), 1.33 (d, J= 7.2 Hz, 3H, CH_3), 1.53 – 1.67 (m, 3H, CH+CH_2), 2.05-2.09 (m, 1H, CH), 3.70 (s, 3H, OCH_3) , 3.95-4.17 (m, 3H, CH_{Val}+CH_{2Gly}),4.53-4.56 (m, 1H, CH_{Ala}), 4.62-4.63 (m, 1H, CH_{Leu}),5.02 (d, J = 12.2 Hz, 1H of CH_2), 5.12 (d, J = 12.1 Hz, 1H of CH_2), 5.82 (d, J = 8.0 Hz, 1H, NH_{Val}),7.28 – 7.33 (m, 5H, ArH), 7.24 (br, IH, NH_{Leu}), 7.36 (br, 1H, NH_{Ala}), 7.53 (br, 1H, NH_{Gly}); ^{13}C NMR (125 MHz, $CDCl_3$) δ 17.7 (+ve, CH_3), 18.0 (+ve, CH_3), 19.1 (+ve, CH_3), 22.1 (+ve, CH_3), 22.7 (+ve, CH), 24.6 (+ve, CH_3), 31.0 (+ve, CH), 41.4 (-ve, CH_2), 42.4 (-ve, CH_2), 47.9 (+ve, CH), 51.7 (+ve, CH), 52.3 (+ve, OCH_3), 60.4 (+ve, CH), 67.0 (-ve, CH_2), 127.9 (+ve, ArCH), 128.1 (+ve, ArCH), 128.5 (+ve, ArCH), 136.1 (ab, ArC), 156.6 (C=O), 168.8 (C=O), 171.8 (C=O), 172.1 (C=O), 173.2 (C=O); HRMS (microTOF-QII, MS, ESI): Calcd for $C_{25}H_{38}N_4O_7$ ($[M+H]^+$) 507.2823, found 507.2813.

4.1.20. N-Cbz-Val-Gly-Leu-Ala-OH (25)

Compound **25** was synthesized according to general procedure B as an oil, yield 22%; $[\alpha]_D^{25}$ = -30° (C=1, $CHCl_3$); ^{1}H NMR (500 MHz, DMSO-d_6, 25 ^{o}C, TMS): δ 0.87-0.95 (m, 12H, 4xCH_3), 1.27 (d, *J* = 7.6 Hz, 3H, CH_3), 1.40–1.47 (m, 2H, CH + 1H of CH_2), 1.59-1.62 (m, 1H, 1H of CH_2), 1.95-1.99 (m, 1H, CH), 3.84.3.87 (m, 1H, CH_{Leu}), 4.23-4.25 (m, 1H, CH_{Ala}), 4.35-4.37 (m, 1H, CH_{Val}), 4.99-5.02 (m, 2H, CH_2), 7.31 (d, *J* = 5.0 Hz, 1H, NH_{Val}), 7.33-7.37 (m, 5H, ArH), 7.84 (d, *J* = 8.5 Hz, 1H, NH_{Leu}), 8.17 (t, *J* = 5.0 Hz, 1H, NH_{Gly}), 8.38 (d, *J* = 6.5 Hz, 1H, NH_{Ala}), 12.47 (br, 1H, OH); ^{13}C NMR (125 MHz, DMSO-d_6) δ 17.1 (+ve, CH_3), 18.6 (+ve, CH_3), 19.4 (+ve, CH_3), 22.2 (+ve, CH_3), 23.4 (+ve, CH), 24.4 (+ve, CH_3), 30.5 (+ve, CH), 41.5 (-ve, CH_2), 42.3 (-ve, CH_2), 47.9 (+ve, CH), 50.9 (+ve, CH), 60.0 (+ve, CH), 65.9 (-ve, CH_2), 128.1 (+ve, ArCH), 128.2 (+ve, ArCH), 128.8 (+ve, ArCH), 137.4 (ab, ArC), 156.7 (C=O), 168.8 (C=O), 172.0 (C=O), 172.2 (C=O), 173.3 (C=O); HRMS (microTOF-QII, MS, ESI): Calcd for $C_{24}H_{36}N_4O_7$ ($[M+Na]^+$) 515.2476, found 515.2517.

4.1.21. N-Cbz Gly-Gly-Phe-Leu-OMe (28)

Compound **28** was synthesized according to general procedure B as white solid; yield 20%, mp 125 ^{o}C, $[\alpha]_D^{25}$ = -20° (C=1, $CHCl_3$); ^{1}H NMR (500 MHz, $CDCl_3$, 25 ^{o}C, TMS): δ 0.86 (d, *J*= 6.3 Hz, 6H, 2xCH_3), 1.48-1.60 (m, 3H, CH+CH_2), 2.97 (dd, *J*= 13.8, 7.1 Hz, 1H, 1H of CH_2), 3.05 (dd, *J*= 13.8, 6.1 Hz, 1H, 1H of CH_2), 3.65 (s, 3H, OCH_3), 3.93-4.02 (m, 4H, 2xCH_2), 4.53-4.57 (m, 1H, CH_{Leu}), 4.96-4.99 (m, 1H, CH_{Phe}), 5.11 (s, 2H, CH_2), 6.02 (t, *J*= 5.02 Hz, 1H, NH_{Gly1}), 7.11-7.20 (m, 5H, ArH), 7.29-7.34 (m, 5H, ArH), 7.35 (br, 1H, NH_{Phe}), 7.38 (d, *J*= 9.3 Hz, 1H, NH_{Leu}), 7.51 (t, *J*= 5.6 Hz, 1H, NH_{Gly2}); ^{13}C NMR (125 MHz, $CDCl_3$) δ 21.9 (+ve, CH_3), 22.6 (+ve, CH), 24.7 (+ve, CH_3), 38.7 (-ve, CH_2), 41.1 (-ve, CH_2), 43.0 (-ve, CH_2), 44.2 (-ve, CH_2), 50.9 (+ve, CH), 52.2 (+ve, OCH_3), 54.2 (+ve, CH), 67.1 (-ve, CH_2), 126.9 (+ve, ArCH), 128.0

(+ve, ArCH), 128.2 (+ve, ArCH), 128.4 (+ve, ArCH), 128.5 (+ve, ArCH), 129.4 (+ve, ArCH), 136.3 (ab, ArC), 156.7 (C=O), 168.5 (C=O), 169.6 (C=O), 170.8 (C=O), 173.0 (C=O);HRMS (microTOF-QII, MS, ESI): Calcd for $C_{28}H_{36}N_4O_7$ ($[M+H]^+$) 541.2656, found 541.2657.

4.1.22. N-Cbz Gly-Gly-Phe-Leu-OH (29)

Compound **29** was synthesized according to general procedure B as a semi-solid; yield 18%, $[\alpha]_D^{25}$ = -40° (C=1, $CHCl_3$); ^{1}H NMR (500 MHz, DMSO-d_6, 25 ^{o}C, TMS): δ 0.85 (d, *J*= 6.5 Hz, 3H, CH_3), 0.90 (d, *J*= 6.6 Hz, 3H, CH_3), 1.52-1.64 (m, 3H, CH+CH_2), 2.75 (dd, *J*= 13.7, 9.1 Hz, 1H, 1H of CH_2), 3.03 (dd, *J*= 13.7, 4.0 Hz, 1H, 1H of CH_2), 3.61-3.69 (m, 4H, 2xCH_2), 4.20-4.24 (m, 1H, CH_{Leu}), 4.54-4.58 (m, 1H, CH_{Phe}), 5.03 (s, 2H, CH_2), 5.16 (br, s, 1H, NH_{Gly1}), 6.33 (t, *J*= 5.0 Hz, 1H, NH_{Gly2}), 7.24-7.35 (m, 10H, ArH), 7.97 (d, *J*= 9.5 Hz, 1H, NH_{Phe}), 8.25 (d, *J*= 9.5 Hz, 1H, NH_{Leu}), 12.47 (br, 1H, OH); ^{13}C NMR (125 MHz, $CDCl_3$) δ 21.8 (+ve, CH_3), 23.3 (+ve, CH), 24.7 (+ve, CH_3), 38.0 (-ve, CH_2), 40.3 (-ve, CH_2), 41.9 (-ve, CH_2), 43.9 (-ve, CH_2), 50.7 (+ve, CH), 54.0 (+ve, CH), 65.9 (-ve, CH_2), 126.7 (+ve, ArCH), 126.8 (+ve, ArCH), 127.0 (+ve, ArCH), 128.1 (+ve, ArCH), 128.2 (+ve, ArCH), 128.4 (+ve, ArCH), 129.6 (+ve, ArCH), 137.4 (ab, ArC), 142.9 (ab, ArC), 158.2 (C=O), 169.9 (C=O), 171.5 (C=O), 172.8 (C=O), 174.3 (C=O); HRMS (microTOF-QII, MS, ESI): Calcd for $C_{27}H_{34}N_4O_7$ ($[M+H]^+$) 527.2496, found 527.2500.

4.1.23. NH_2 Gly-Gly-Phe-Leu-OMe (30)

Compound **30** was synthesized according to general procedure B and C as white solid; yield 22%, mp 78 ^{o}C, $[\alpha]_D^{25}$ = -50° (C=1, MeOH); ^{1}H NMR (500 MHz, DMSO-d_6, 25 ^{o}C, TMS): δ 0.84 (d, *J*= 6.4 Hz, 3H, CH_3), 0.90 (d, *J*= 6.4 Hz, 3H, CH_3), 1.48-1.64 (m, 3H, CH+CH_2), 2.76 (dd, *J*= 13.8, 9.2 Hz, 1H, 1H of CH_2), 3.05 (dd, *J*= 13.8, 4.8 Hz, 1H, 1H of CH_2), 3.15 (br, 2H, CH_2), 3.61 (s, 3H, OCH_3), 3.63 (br, 1H, 1H of CH_2), 3.72-3.76 (m, 1H, 1H of CH_2), 4.26-4.30

(m, 1H, CH_{Leu}), 4.53-4.57 (m, 1H, CH_{Phe}), 7.17-7.27 (m, 5H, ArH), 8.11 (br, 1H, NH_{Gly}), 8.17 (d, *J*= 8.2 Hz, 1H, NH_{Phe}), 7.51 (d, *J*= 7.6 Hz, 1H, NH_{Leu}); ^{13}C NMR (125 MHz, normal/DEPT-135) δ 21.6 (+ve, CH_3), 23.2 (+ve, CH), 24.6 (+ve, CH_3), 37.9 (-ve, CH_2), 40.4 (-ve, CH_2), 42.1 (-ve, CH_2), 44.6 (-ve, CH_2), 50.8 (+ve, CH), 52.3 (+ve, OCH_3), 54.0 (+ve, CH), 126.7 (+ve, ArCH), 128.4 (+ve, ArCH), 129.6 (+ve, ArCH), 138.2 (ab, ArC), 168.9 (C=O), 171.7 (C=O), 173.0 (C=O), 173.2 (C=O),; HRMS (microTOF-QII, MS, ESI): Calcd for $C_{20}H_{30}N_4O_5$ ($[M+H]^+$) 407.2288, found 407.2351.

4.1.24. NH_2 Gly-Gly-Phe-Leu-OH (31)

Compound **31** was synthesized according to general procedure B and C as a semi-solid; yield 20%, $[\alpha]_D^{25}$ = -30° (C=1, MeOH); ^1H NMR (500 MHz, DMSO-d_6, 25 °C, TMS): δ 0.83 (d, *J*= 6.8 Hz, 3H, CH_3), 0.88 (d, *J*= 6.3 Hz, 3H, CH_3), 1.48-1.63 (m, 3H, CH+CH_2), 2.74 (dd, *J*= 13.9, 9.7 Hz, 1H, 1H of CH_2), 3.01 (dd, *J*= 13.9, 4.5 Hz, 1H, 1H of CH_2), 3.14 (br, 2H, CH_2), 3.71-3.74 (m, 2H, CH_2), 4.24-4.29 (m, 1H, CH_{Leu}), 4.52-4.56 (m, 1H, CH_{Phe}), 7.16-7.26 (m, 5H, ArH), 8.10 (br, 1H, NH_{Gly}), 8.16 (d, *J*= 8.1 Hz, 1H, NH_{Phe}), 8.40 (d, *J*= 7.5 Hz, 1H, NH_{Leu}); ^{13}C NMR (125 MHz, normal/DEPT-135) δ 22.0 (+ve, CH_3), 23.4 (+ve, CH), 24.8 (+ve, CH_3), 38.2 (-ve, CH_2), 40.6 (-ve, CH_2), 42.3 (-ve, CH_2), 44.9 (-ve, CH_2), 51.0 (+ve, CH), 54.2 (+ve, CH), 126.9 (+ve, ArCH), 128.7 (+ve, ArCH), 129.9 (+ve, ArCH), 138.4 (ab, ArC), 169.2 (C=O), 171.9 (C=O), 173.2 (C=O), 173.4 (C=O),; HRMS (microTOF-QII, MS, ESI): Calcd for $C_{19}H_{28}N_4O_5$ ($[M+H]^+$) 393.2132, found 393.2122.

4.2. Docking Procedure

The molecular docking was performed using Schrodinger (Schrödinger Release 2014-4: Maestro, version 10.0, Schrödinger, LLC, New York, NY, 2014). Crystal co-ordinates of COX-2 (PDB ID 1CVU) were downloaded from the protein data bank (www.rcsb.org). In the first step,

bond orders were assigned and hydrogens were added by preprocess option. Excess water molecules were deleted. The hetero atoms were ionized by epik[54,55] at biological pH to consider the protein permeability and drug solubility and then the H-Bonds were optimized to reduce the steric clashes by histidine, aspartate, glutamate, and hydroxyl containing amino acids. Then complete protein structure was minimized by using OPLS 2005 force field.[56-58] Ligand preparation is generally required because molecules lack 3D coordinates, ionization, stereochemistry and tautomers. Thus before docking the least energy state of ligand was needed to be prepared. Ligprep tool of Schrödinger was used to prepare the least energy state of ligand which converts 1D/2D structures to 3D. Finally, this ligand molecule was minimized with the help of the OPLS 2005 force field. For docking, the grids were generated by using the grid-based energy descriptor which had a default set of options with Van der Waals radius of 1.0. These grids were then used to calculate the interaction of prepared ligand with the receptor using the XP ligand docking in glide. Thus H-bonding, hydrophobic interactions and π-π stacking between enzyme and compound were determined.

3D-QSAR analysis was performed using field-based QSAR tool of Schrodinger 2014-4. CoMFA (Comparative Molecular Field Analysis) describes correlation between biological activity of a set of molecules and their 3-D shape, electrostatic and H-bonding characteristics. All the compounds used in the 3-D QSAR studies were synthesized and evaluated for anti-inflammatory activity. The IC_{50} values of all compounds for COX-2 inhibition were normalized and converted to the logarithm unit of molar grade ($pIC_{50}= -logIC_{50}$).

For the generation of field-based 3D-QSAR models the molecules were aligned on the basis of common scaffold. Out of 22 compounds, 16 compounds were selected randomly as training set for model construction and the remaining 6 were used as test set for model validation, according

to the biological activity and structural diversity. By using PLS with three factors, the field-based QSAR model was generated by correlating with five fields: steric, electrostatic, hydrophobic, HBD and HBA.

4.3. Procedure for COX-1/2 inhibitory immunoassay

In vitro COX-1 and COX-2 inhibitory activities were evaluated using "COX inhibitor screening assay" according to the manufacturer's instructions. The enzymes were ovine COX-1 and human recombinant COX-2. Each compound was tested in triplicate at each concentration and the percentage inhibition for COX-1/2 was obtained for each experiment. The difference between the values of the three experiments was <3%. For calculating the IC_{50}, average of the three percentage inhibitions of each concentration of the compound was taken. The amount of prostaglandins produced by each enzyme in the presence of various concentrations of the test compounds was measured and compared with the control experiments (also performed in triplicate).

Enzyme inhibition = 1/conc of prostaglandin in each enzymatic reaction

The background samples were prepared for both COX-1 and COX-2 by taking 20 µl of each enzyme in separate test tubes and keeping them in boiling water for 3 min. The background tubes for COX-1 and COX-2 were prepared by adding 970 µl of reaction buffer, 10 µl of heme and 10 µl of inactive COX-1 or COX-2. COX-1 and COX-2 initial activity tubes were prepared taking 950 µL of reaction buffer, 10 µL of heme, 10 µL of COX-1 and COX-2 enzymes into respective tubes. Inhibitor tubes were prepared for all test compounds. COX-1/COX-2 inhibitor tubes were prepared by adding 950 µL of reaction buffer, 10 µL of heme, 10 µL of COX-1/COX-2, 20 µL of inhibitor solution. After incubation of the tubes at 37 ^{o}C for 10 min, 10 µL of arachidonic acid was added to all tubes and were incubated at 37 ^{o}C for 2 min. The reaction was quenched with 30

μL of saturated $SnCl_2$ to each reaction tube. The prostaglandins produced in each well were quantified using EIA. Prostaglandin screening standards were prepared as test tubes S1-S8. 800 μl of EIA buffer was added to S1 and 500 ml of the same was added to S2-S7. Then 200 μl of bulk standard (10 ng/ml) was added to tube S1 and mixed thoroughly. The standards were diluted serially by removing 500 μl from tube S1 and placing it in tube S2 and mixed thoroughly. Same process was repeated from S2-S3, up to S7-S8. To make dilutions for COX reactions, test tubes BC1 and BC2 were prepared by adding 990 μl of EIA (enzyme immunoassay) buffer and 10 μl of background COX-1 or COX-2 and mixed thoroughly. COX 100% initial activity samples were prepared as three test tubes for COX-1 and COX-2 both and labelled as IA1-IA3. For each sample, aliquot 990 μl of EIA buffer to IA1, 950 μl of EIA buffer to IA2 and 500 μl of EIA buffer to IA3. 10 μl of COX-1/COX-2 100% initial activity sample was added to IA1 and mixed thoroughly. Aliquot, 50 μl of tube IA1 and added to tube IA2 and mixed thoroughly. Again aliquot 500 ml from test tube IA2 and added to test tube IA3 and mixed well. In the same manner, COX inhibitor samples were prepared by further dilutions and named C1-C3 for each concentration. After the dilutions, these solutions were introduced on 96 well plate. The plate contains two blank wells- 1A, 1B; two NSB (Non-specific binding)- 1C, 1D; and two Bo (Maximum binding)- 1E, 1F. Well 1H was named as TA (Total activity well). Wells 2A-2H were used for S1- S8 and 3A-3H were used for S1-S8 duplicate. Wells 4A and 5A were prepared as BC1 and its duplicate. Similarly, for BC2 wells 4B and 5B were prepared. Remaining wells were used for inhibitor samples for COX-1 and COX-2. Then Addition of the reagents on 96-well plate was performed. 100 μl EIA buffer was added to NSB well and 50 μl of EIA buffer was added to Bo well. 50 μl of Prostaglandin screening standard was added to the respective wells S1-S8 from their respective test tubes S1-S8 and duplicated. 50 μl of BC1 and BC2 were added

per well and in duplicate. 50 µl of 100% initial activity samples were added per well and only IA2 and IA3 were assayed in duplicate for both COX-1 and COX-2. 50 µl of COX inhibitor samples were added per well from their respective dilutions (only C2 and C3 were assayed). 50 µl of PG screening AchE tracer was added to each well except TA and Blank well. At last, 50 µl of PG screening EIA antiserum was added to each well except TA, NSB and blank wells. The plate was then covered with plastic film and was incubated for 18 h at room temperature. After incubation, the plate was developed by emptying the wells and rinsing the wells for five times with wash buffer. Then 200 µl of Ellman's reagent was added to each well and 5 ml of tracer was added to Total activity well. The plate was covered with plastic film and was kept for 60-90 min. Finally the plate was read at 420 nm and the COX inhibitory activities of the compounds were quantified from the absorbance values of different wells of the 96-well plates. The concentrations of the test compound causing 50% inhibition (IC_{50}) were determined using a dose response inhibition curve (duplicate determinations) with GraphPad PRISM.

4.4. 5-LOX inhibition by compound 30. Same procedure as described previously[37] was used for screening of compound **30** for 5-LOX inhibition.

4.5. Human Whole Blood Assay. The whole blood was stimulated with calcium ionophore (A23187), and lipopolysaccharide (LPS) and the release of TxB_2 and PGE_2 was measured using an enzyme-linked immunosorbent assay (ELISA)- TXB_2 Express ELISA kit and COX inhibitor screening assay kit respectively.

Sample preparation

Blood of a healthy volunteer was collected by venipuncture into EDTA tubes. For COX-1 assay, blood samples (1 ml) were treated with 100 µL of compound **30**/ indomethacin/ vehicle (DMSO) (final conc 1 µM), followed 60 min later by addition of 100 µL of calcium ionophore, A23187

(final conc 50 μM) into each sample. After 30 min, all the samples were centrifuged (1500 x g, 4 ^{o}C, 5 min), the plasma was removed and frozen. All the samples were prepared in duplicate. TxB_2 (the breakdown product of TxA_2) was quantified by ELISA, TxB_2 Express ELISA kit (Cayman Chemicals, Ann Arbor, MI).

For COX-2 assay, the blood samples (800 μL each) were treated with 50 μL acetylsalicyclic acid (final concentration = 10 μg/ml) to inactivate COX-1. Then all the samples were incubated for 6 h. After incubation 100 μL of compound **30**/ indomethacin/ vehicle (DMSO) (final conc 1 μM) was added followed 15 min later by addition of 50 μL of LPS solution (final concentration = 10 μg/ml) and incubated for 18 h. After 18 h, samples were centrifuged (1000 x g, 4 ^{o}C, 15 min), and the plasma was removed and stored at -20 ^{o}C. PGE_2 concentrations in all the samples were determined by using an enzyme-linked immunosorbent assay (ELISA), COX inhibitor screening assay kit.

TxB_2, the breakdown product of TxA_2, was quantified in the final supernatant using "TXB_2 Express ELISA kit" according to the manufacturer's instructions (Cayman Chemicals, Ann Arbor, MI). This assay measures the amount of thromboxane B_2 in serum in the presence of compound **30** and compared with control experiments.

$$\text{Absorbance} = 1/\ [TxB_2]$$

TxB_2 Express standards were prepared as test tubes S1-S8. 900 μl of EIA buffer was added to S1 and 500 ml of the same was added to S2-S7. Then 100 μl of bulk standard (20 ng/ml) was added to tube S1 and mixed thoroughly. The standards were diluted serially by removing 500 μl from tube S1 and placing it in tube S2 and mixed thoroughly. Same process was repeated from S2-S3, up to S7-S8. After the dilutions, these solutions were introduced on 96 well plate. The plate contains two blank wells-1A, 1B; two NSB (Non-specific binding)-1C, 1D; and two Bo

(Maximum binding)-1E, 1F. Well 1H was named as TA (Total activity well). Wells 2A-2H were used for S1- S8 and 3A-3H were used for S1-S8 duplicate. Wells 4A-4C were used for the quantification of TxB_2 obtained in the presence of compound **30**. 100 µl EIA buffer was added to NSB well and 50 µl of EIA buffer was added to Bo well. 50 µl of TxB_2 express ELISA standard was added to the respective wells S1-S8 from their respective test tubes S1-S8 and duplicated. 50 µl of serum sample was added to the wells 4A-4C. 50 µl of TxB_2 express AchE tracer was added to each well except TA and Blank well. At last, 50 µl of TxB_2 express ELISA Monoclonal Antibody was added to each well except TA, NSB and blank wells. The plate was then covered with plastic film and was incubated for 2 h at room temperature. After incubation, the plate was developed by emptying the wells and rinsing the wells for five times with wash buffer. Then 200 µl of Ellman's reagent was added to each well and 5 ml of tracer was added to Total activity well. The plate was covered with plastic film and was kept for 60-90 min. Finally the plate was read at 420 nm and the TxB_2 production was quantified from the absorbance values of different wells of the 96-well plate. A standard curve was obtained using the range of concentrations of TxB_2 (0, 15.6, 31.3, 62.5, 125, 250, 500, 1000 and 2000 pg/mL). The concentrations of TxB_2 in the calcium ionophore stimulated whole blood in the presence of compound **30** were determined. The quantification of PGE_2 (as a measure of COX-2 activity) was performed in a similar way as described in section 4.3 for enzyme immunoassay. This assay measures the amount of PGE_2 in serum obtained in the presence of compound **30** and comparing with control experiments.

4.6. Analgesic and anti-inflammatory activity

Swiss albino mice of either sex (25–35 g) were used in the present study. The animals were maintained at 22 ± 2 °C under 12 h light/12 h dark cycle with free supply of food and water. The study has been approved by the IAEC of Guru Nanak Dev University, Amritsar, Punjab, India. A

total of fifteen groups with 5 animals in each group were used in the current investigation. The experimental procedure as depicted in Figure 1 and Figure 2 and described in our previous report[37,44] was used for studying the analgesic and anti-inflammatory activity of the compounds.

Mechanistic studies. Six groups of mice with 5 animals in each group were taken for exploring the inhibition of COX and LOX, modulation of nitric oxide pathway, voltage gated sodium channels (VGSC), calcium and potassium channels. For COX-LOX pathway, the animals were pretreated with substance P, 30 min before administering compound **30**. For nitric oxide pathway, animals were pretreated with nitric oxide precursor, L-arginine and NOS inhibitor, L-NAME, 30 min before administering compound **30**. For modulation of VGSC, veratrine, a VGSC opener was administered, calcium influx was induced by administering A23187, a calcium ionophore and for modulation of potassium channels, glipizide, an inhibitor of ATP sensitive potassium channels was given 30 min before compound **30**. The details of the protocols are shown in figure 2.

Acute Toxicity Studies. Four groups of animals with three animals per group were taken. The first group was administered the vehicle and served as the control group, the second, third and the fourth groups were treated with compound **30** at doses of 50 mg Kg^{-1}, 300 mg Kg^{-1} and 2000 mg Kg^{-1} respectively. All the treatments were administered after 4 h of fasting. Thereafter, the animals were observed continuously for the first four hours and periodically for 24 h. After 14 days, one animal each in control and highest dose (2000 mg Kg^{-1}) was sacrificed and histological studies were conducted using H and E staining.

4.7. Isothermal titration calorimetric experiments. The stock solution of compound **30** (100 μM) was prepared in the HPLC grade ethanol and HEPES buffer (1:99) (pH 7.4). The stock solution of enzymes were prepared by dissolving 10 μl of enzyme in 5 ml of HEPES buffer. The

compound solution was taken in a rotating stirrer syringe (500 rpm) and titrated into the sample cell containing the enzyme in HEPES buffer. The experiment was performed in triplicate and the difference between the values from different experiments was <1%. Each experiment consisted of 19 consecutive injections of 2 μL of the compound to the enzyme in the sample cell after regular time intervals of 120 s so that the equilibrium is attained in each titration point. Control experiments in triplicate were performed for comparison. The total heat Q produced or absorbed in the active cell volume V_o determined at fractional saturation Q after the ith injection. The control titrations consisting identical titrant solution with the same cell filled just with the buffer solution and also the successive buffer additions to the enzyme solution were carried out to determine the background heat which was to be subtracted from the main experiment. This was done just to eliminate heat of mixing and heat of dilution. The origin 7.0 software by Microcal was used to read the titration heat profiles for calculating the binding parameters. The single binding site model was used to fit the data.

ASSOCIATED CONTENT

Supporting information

^{1}H and ^{13}C NMR spectra, Mass Spectra and Molecular Docking Data. This material is available free of charge via the Internet at http://pubs.acs.org.

PDB Coordinates for Computational Models

Three-dimensional model of target–ligand (compound **6**/**30** docked in COX-1/2 and compound **30** docked in iNOS) complexes are given as PDB-formatted coordinate files in the supporting information.

Homology Models: NA

Molecular formula strings (CSV)

AUTHOR INFORMATION

Corresponding Author

Palwinder Singh, Department of Chemistry, Guru Nanak Dev University, Amritsar-143005. India; e-mail: palwinder_singh_2000@yahoo.com

ACKNOWLEDGMENTS

Financial assistance from CSIR, New Delhi is gratefully acknowledged. SK thanks CSIR, New Delhi for SRF and JK thanks DST, New Delhi for SRF. UGC, New Delhi is gratefully acknowledged for grant to GNDU under University with Potential for Excellence Programme.

ABBREVIATIONS

IC_{50}, Inhibitory Concentration at 50% inhibition; COX-2, Cyclooxygenase-2; COX-1, Cyclooxygenase-1; AA, arachidonic acid; DMSO, dimethyl sulphoxide; ACN, acetonitrile; DMF, dimethylformamide; TFA, trifluoro acetic acid; TLC, thin layer chromatography; HRMS, High resolution mass spectrometry; TPSA, total polar surface area; SEM, standard error mean; i.p., intraperitoneally; iNOS, Induced nitric oxide synthetase; ECF, Ethyl chloroformate; Cbz, benzyl chloroformate; VGSC, voltage gated sodium channels; L-NAME, N-Nitro-L-arginine methyl ester

References

1. Cloutheir, C. M.; Pelleteir, J. N. Expanding the organic toolbox: A guide to integrating biocatalysis in synthesis. *Chem. Soc. Rev*. **2012**, *41*, 1585-1605.

2. Kaur, N.; Lu, X.; Gerhengorn, M. C.; Jain, R. Thyrotropin-releasing hormone (TRH) analogues that exhibit selectivity to TRH receptor subtype 2. *J. Med. Chem*. **2005**, *48*, 6162-6165.

3. Rivier, J.; Vale, W.; Monahan, M.; Ling, N.; Burgus, R. Synthetic thyrotropin-releasing factor analogs.3. Effect of replacement or modification of histidine residue on biological activity. *J. Med. Chem*. **1972**, *15*, 479-482.

4. Pearce, T. R.; Shroff, K.; Kokkoli, E. Peptide targeted lipid nanoparticles for anticancer drug delivery. *Adv. Mater*. **2012**, *24*, 3803-3822.

5. Eliassen, L. T.; Berge, G.; Sveinbjornsson, B.; Svendsen, J. S.; Vorland, L. H.; Rekdal, O. Evidence for a direct antitumor mechanism of action of bovine lactoferricin. *Anticancer Res*. **2002**, *22*, 2703-2710.

6. Baggio, L. L.; Huang, Q.; Brown, T. J.; Drucker, D. J. A recombinant human glucagon-like peptide (GLP)-1-albumin protein (albugon) mimics peptidergic activation of GLP-1 receptor-dependent pathways coupled with satiety, gastrointestinal motility and glucose homeostasis. *Diabetes* **2004***, 53*, 2492-2500.

7. Xiao, Q.; Giguere, J.; Parisien, M.; Jeng, W.; St-Pierre, S. A.; Brubaker, P. L.; Wheeler, M. B. Biological activities of glucagon-like peptide-1 analogues in vitro and in vivo. *Biochemistry* **2001**, *40*, 2860-2869.

8. Fiell, C. D.; Hiss, J. A.; Hancock, R. E. W.; Schneider, G. Designing antimicrobial peptides: Form follows function. *Nat. Rev. Drug Discov.* **2012**, *11*, 37-51.

9. Matsunaga, S.; Fusetani, N.; Hashimoto, K.; Walchli, M. Theonellamide F. A novel antifungal bicyclic peptide from a marine sponge *Theonella sp*. *J. Am. Chem. Soc*. **1989**, *111*, 2582-2588.

10. Craik, D. J.; Fairlie, D. P.; Liras, S.; Price, D. The future of peptide-based drugs. *Chem. Biol. Drug. Des.* **2013**, *81*, 136-147.

11. Uhlig, T.; Kyprianou, T.; Martinelli, F. G.; Oppici, C. A.; Heiligers, D.; Hills, D.; Calvo, X. R.; Verhaert, P. The emergence of peptides in the pharmaceutical business: From exploration to exploitation. *EuPa. Open Proteomics* **2014**, ***4***, 58-69.

12. Fosgerau, K.; Hoffmann, T. Peptide therapeutics: current status and future directions. *Drug Discov. Today*, **2015**, *20*, 122-128.

13. Needleman, P.; Truk, J.; Jakschik, B. A.; Morrison, A. R.; Lefkowith, J. B. Arachidonic acid metabolism. *Ann. Rev. Biochem.* **1986**, *55*, 69-102.

14. Smith, W. L.; Garavito, R. M.; DeWitt, D. L. Prostaglandin endoperoxide H synthases (cyclooxygenases)-1 and -2. *J. Biol. Chem.* **1996**, *52*, 33157-33160.

15. Dubois, R. N.; Abramson, S. B.; Crofford, L.; Gupta, R. A.; Simon, L. S.; Van De Putte, L. B. A.; Lipsky, P. E. Cyclooxygenase in biology and disease. *The FASEB Journal* **1998**, *12*, 1063-1073.

16. Marnett, L. J.; Rowlinson, S. W.; Goodwin, D. C.; Kalgutkar, A. S.; Lanzo, C. A. Arachidonic acid oxygenation by COX-1 and COX-2. *J. Biol. Chem.* **1999**, *274*, 22903-22906.

17. Garavito, R. M.; DeWitt, D. L. The cyclooxygenase isoforms: structural insights into the conversion of arachidonic acid to prostaglandins. *Biochim. Biophys. Acta* **1999**, *1441*, 278-287.

18. Simmons, D. L.; Botting, R. M.; Hla, T. Cyclooxygenase Isozymes: The biology of prostaglandin synthesis and inhibition. *Pharmacol. Rev.* **2004**, *56*, 387-437.

19. Ricciotti, E.; FitzGerald, G. A. Prostaglandins and inflammation. *Arterioscler. Thromb. Vasc. Biol.* **2011**, *31*, 986-1000.

20. Patrono, C.; Baigent, C. Low-dose aspirin, coxibs, and other NSAIDS: A clinical mosaic emerges. *Mol. Interventions*, **2009**, *9*, 31-39.

21. Skoutakis, V. A.; Carter, C. A.; Mickle, T. R.; Smith, V. H.; Arkin, C. R.; Alissandratos, J.; Petty, D. E. Review of diclofenac and evaluation of its place in therapy as a nonsteroidal anti-inflammatory agent. *Drug Intell. Clin. Pharm.* **1988**, *22*, 850-859.

22. Brunton, L.; Chabner, B.; Knollman, B. Anti-inflammatory, Antipyretic and Analgesic Agents. In *The Pharmacological Basis of Therapeutics*, 12th ed.; Goodman, L. S.; Gilman, A., Eds.; MacGraw-Hill Inc, New York, ch-34, pp 959-1003.

23. Shi, S.; Klotz, U. Clinical use and pharmacological properties of selective COX-2 inhibitors. *Eur. J. Clin. Pharmacol.* **2008**, *64*, 233-252.

24. Chan, F. K. L.; Hung, L. C. T.; Suen, B. Y.; Wu, J. C. Y.; Lee, K. C.; Leung, V. K. S.; Hui, A. J.; Leung, W. L.; Wong, V. W. S.; Chung, S. C. S.; Sung, J. J. Y. Celecoxib versus diclofenac and omeprazole in reducing the risk of recurrent ulcer bleeding in patients with arthritis. *N. Engl. J. Med.* **2002**, *26*, 2104-2110.

25. Moore, R. A.; Derry, S.; Phillips, C. J.; McQuay, H. J. Nonsteroidal anti-inflammatory drugs (NSAIDs), cyclooxygenase-2 selective inhibitors (coxibs) and gastrointestinal harm: review of clinical trials and clinical practice. *BMC Musculoskelet. Disord.* **2006**, *7*, 79-92.

26. Capone, M. L.; Tacconelli, S.; Sciulli, M.G.; Patrignani, P. Clinical pharmacology of selective COX-2 inhibitors. *Int. J. Immunopathol. Pharmacol.* **2003**, *16*, 49-58.

27. Dogne, J-M.; Supuran, C. T.; Pratico, D. Adverse cardiovascular effects of the coxibs. *J. Med. Chem.* **2005**, *48*, 2251-2256.

28. Kawahito, Y. Clinical implications of cyclooxygenase-2 inhibitors. *Inflamm. Regen.* **2007**, *27*, 552-558.

29. White, W. B.; West, C. R.; Borer, J. S.; Gorelick, P. B.; Lavange, L.; Pan, S. X.; Weiner, E.; Verburg, K. M. Risk of cardiovascular events in patients receiving celecoxib: A meta-analysis of randomized clinical trials. *Am. J. Cardiol.* **2007**, *99*, 91-98.

30. Bruggemann, L. I.; Mackie, A. R.; Mani, B. K.; Cribbs, L. L.; Byron, K. L. Differential effects of selective cyclooxygenase-2 inhibitors on vascular smooth muscle ion channels may account for differences in cardiovascular risk profiles. *Mol. Pharmacol.* **2009**, *76*, 1053-1061.

31. FitzGerald, G. A. Cardiovascular pharmacology of nonselective nonsteroidal anti-inflammatory drugs and coxibs: Clinical considerations. *Am. J. Cardiol.* **2002**, *89*, 26-32.

32. Solomon, S. D.; McMurray, J. J. V.; Pfeffer, M. A.; Wittes, J.; Fowler, R.; Finn, P.; Anderson, W. F.; Hawk, E.; Bertagnolli, M. Cardiovascular risk associated with celecoxib in a clinical trial for colorectal adenoma prevention. *N. Engl. J. Med.* **2005**, *352*, 1071-1080.

33. Cairns, J. A. The coxibs and traditional nonsteroidal anti-inflammatory drugs: A current perspective on cardiovascular risks. *Can. J. Cardiol.* **2007**, *23*, 125-131.

34. Klementiev, B.; Li, S.; Korshunova, I.; Dmytriyeva, O.; Pankratova, S.; Walmod, P. S.; Kjær, L. K.; Dahllöf, M. S.; Lundh, M.; Christensen, D. P.; Mandrup-Poulsen, T. Anti-inflammatory properties of a novel peptide interleukin I receptor antagonist. *J. Neuroinflammation* **2014**, *11*:27, 1-18.

35. Veljaca, M. Anti-inflammatory peptides and proteins in inflammatory bowel disease. *Curr. Opin. Invest. Drugs* **2001**, *10*, 1387-1394.

36. Dellai, A.; Maricic, I.; Kumar, V.; Arutyunyan, S.; Bouraoui, A.; Nefzi, A. Parallel synthesis and anti-inflammatory activity of cyclic peptides cyclosquamosin D and Met-cherimolacyclopeptide B and their analogs. *Bioorg. Med. Chem. Lett*. **2010**, *20*, 5653-5657.

37. Singh, P.; Prasher, P.; Dhillon, P.; Bhatti, R. Indole based peptidomimetics as anti-inflammatory and antihyperalgesic agents: Dual inhibition of 5-LOX and COX-2 enzymes. *Eur. J. Med. Chem*., **2015**, *97*, 104-123.

38. Picot, D.; Loll, P. J.; Garavito, R. M. The X-ray crystal structure of the membrane protein prostaglandin H_2 synthase-1. *Nature* **1994**, *367*, 243-249.

39. Vecchio, A. J.; Simmons, D. M.; Malkowski, M. G. Structural basis of fatty acid substrate binding to cyclooxygenase-2. *J. Biol. Chem.* **2010**, *285*, 22152-22163.

40. Rowlinson, S. W.; Crews, B. C.; Lanzos, C. A.; Marnett, L. J. The binding of arachidonic acid in the cyclooxygenase active site of mouse prostaglandin endoperoxide synthase-2 (COX-2). *J. Biol. Chem.* **1999**, *274*, 23305-23310.

41. COX Inhibitor Screening Assay kit, Item No. 560131. Cayman Chemical Co.

42. Warner, T. D.; Giuliano, F.; Vojnovic, I.; Bukasa, A.; Mitchell, J. A. Nonsteroid drug selectivities for cyclo-oxygenase-1 rather than cyclo-oxygenase-2 are associated with human gastrointestinal toxicity: A full in vitro analysis. *Proc. Natl. Acad. Sci*. **1999**, *96*, 7563-7568.

43. Laufer, S.; Greim, C.; Luik, S.; Ayoub, S. S.; Dehner, F. Human whole blood assay for rapid and routine testing of non-steroidal anti-inflammatory drugs (NSAIDs) on cyclo-oxygenase-2 activity. *Inflammopharmacology* **2008**, *16*, 155-161.

44. Singh, P.; Kaur, H.; Singh, G, Bhatti, R. Tri-block conjugates: Identification of a highly potent anti-inflammatory agent. *J. Med. Chem*. **2015**, *58,* 5989–6001.

45. Hunskaar S, Hole K. The formalin test in mice: dissociation between inflammatory and non-inflammatory pain. *Pain* **1987**, *30*, 103-114.

46. Koon, H. W.; Zhao, D.; Zhan, Y.; Rhee, S. H.; Moyer, M. P.; Pothoulakis, C. Substance P stimulates cyclooxygenase-2 and prostaglandin E2 expression through JAK-STAT activation in human colonic epithelial cells. *J. Immunol.* **2006**, *176*, 5050-5059.

47. Castellani, M. L.; Conti, P.; Felaco, M.; Vecchiet, J.; Ciampoli, C.; Cerulli, G.; Boscolo, P.; Theoharides, T. C. Substance P upregulates LTB_4 in rat adherent macrophages from granuloma induced by $KMnO_4$. *Neurotox. Res.* **2009**, *15*, 49-56

48. Ge, Z. J; Tan, Y. F; Zhao, Y. P; Cui, G. X. Evidence that inhibition of spinal nitric oxide production contributes to the antinociceptive effects of emulsified isoflurane on formalin-induced pain in rats. *Clin. Exp. Physiol. Pharmacol*. **2008**, *35*, 245-1251.

49. Knapp, O.; McArthur, J. R.; Adams, D. J. Conotoxins targeting neuronal volage gated sodium channel subtypes: potential analgesics? *Toxins*, **2012**, *4*, 1236-1260.

50. Comunanza, V.; Carbone, E.; Marcantoni, A.; Sher, E.; Ursu, D. Calcium dependent inhibition of T-type calcium channels by TRPV1 activation in rat sensory neurons. *Pflug. Arch. Eur. J. Phy*. **2011**, *462*, 709-722.

51. Hayashi, Y.; Kawaji, K.; Sun, L.; Inoue, K.; Nakanishi, H. Microglial Ca^{2+} activated K^{+} channels are possible molecular targets for the analgesic effects of S-ketamine on neuropathic pain. *J. Neurosci.* **2011**, *31*, 17370-17382.

52. OECD Guideline for testing of chemicals, 2001. Guideline 423: acute oral toxicity- acute toxic class method, 2001.

53. Kiefer, J. R.; Pawlitz, J. L.; Moreland, K. L.; Stegeman, R. A.; Hood, W. F.; Gierse, J. K.; Stevens, A. M.; Goodwin, D. C.; Rowlinson, S. W.; Marvnett, L. J.; Stallings, W. C.; Kurumbail, R. G. Structural insights into the stereochemistry of the cyclooxygenase reaction. *Nature* **2000**, *405*, 97-101.

54. Greenwood, J. R.; Calkins, D.; Sullivan, A. P.; Shelley, J. C. Towards the comprehensive, rapid, and accurate prediction of the favorable tautomeric states of drug-like molecules in aqueous solution. *J. Comput. Aided Mol. Des.* **2010**, *24*, 591-604.

55. Shelley, J.C.; Cholleti, A.; Frye, L; Greenwood, J.R.; Timlin, M.R.; Uchimaya, M. Epik: a software program for pK_a prediction and protonation state generation for drug-like molecules. *J. Comp. Aided Mol. Des.* **2007**, *21*, 681-691.

56. Shivakumar, D.; Williams, J.; Wu, Y.; Damm, W.; Shelley, J.; Sherman, W. Prediction of absolute solvation free energies using molecular dynamics free energy perturbation and the OPLS force field. *J. Chem. Theory Comput.* **2010**, *6*, 1509–1519.

57. Jorgensen, W.L.; Maxwell, D.S.; Tirado-Rives, J. Development and testing of the OPLS all-atom force field on conformational energetics and properties of organic liquids. *J. Am. Chem. Soc.* **1996**, *118*, 11225-11236.

58. Jorgensen, W. L.; Tirado-Rives, J. The OPLS [optimized potentials for liquid simulations] potential functions for proteins, energy minimizations for crystals of cyclic peptides and crambin. *J. Am. Chem. Soc.* **1988**, *110*, 1657-1666.

59. Rowlinson, S. W.; Kiefer, J. R.; Prusakiewicz, J. J.; Pawlitz, J. L.; Kozak, K. R.; Kalgutkar, A. S.; Stallings, W. C.; Kurumbail, R. G.; Marnett, L. J. A novel mechanism of cyclooxygenase-2 inhibition involving interactions with ser-530 and tyr-385. *J. Biol. Chem.* **2003**, *278*, 45763-45769.

60. Shimokawa, T.; Kulmacz, R. J.; DeWitt, D. L.; Smith, W. L. Tyrosine 385 of prostaglandin endoperoxide synthase is required for cyclooxygenase catalysis. *J. Biol. Chem.* **1990**, *265*, 20073-20076.

61. Mancini, J. A.; Riendeau, D.; Falgueyret, J-P.; Vickers, P. J.; Neill, G. P. O. Arginine 120 of prostaglandin G/H synthase-1 is required for the inhibition by nonsteroidal Anti-inflammatory drugs containing a carboxylic acid moiety. *J. Biol. Chem.* **1995**, *270*, 29372-29377.

62. Bhattacharyya, D. K.; Lecomte, M.; Rieke, C. J.; Garavitto, R. M.; Smith, W. L. Involvement of arginine 120, glutamate 524, and tyrosine 355 in the binding of arachidonate and 2-phenylpropionic acid inhibitors to the cyclooxygenase active site of ovine prostaglandin endoperoxide H synthase-1. *J. Biol. Chem.* **1996**, *271*, 2179-2184.

63. Rieke, C. J.; Mulichak, A. M.; Garavito, R. M.; Smith, W. L. The role of arginine 120 of human prostaglandin endoperoxide H synthase-2 in the interaction with fatty acid substrates and inhibitors. *J. Biol. Chem.* **1999**, *274*, 17109-17114.

64. Garcin, E. D.; Arvai, A. S.; Rosenfeld, R. J.; Kroeger, M. D.; Crane, B. C.; Andersson, G.; Andrews, G.; Hamley, P. J.; Mallinder, P. R.; Nicholls, D. J.; St-Gallay, S. A.;

Tinker, A. C.; Gensmantel, N.P.; Mete, A.; Cheshire, D.R.; Connolly, S.; Stuehr, D. J.; Åberg, A.; Wallace, A.V.; Tainer, J. A.; Getzoff, E. D. Anchored plasticity opens doors for selective inhibitor design in nitric oxide synthase. *Nat. Chem. Biol.* **2008**, *4*, 700 – 707.

65. Pauli, G. F.; Chen, S-N.; Simmler, C.; Lankin, D. C.; Godecke, T.; Jaki, B. U.; Friesen, J. B.; McAlpine, J. B.; Napolitano, J. G. Importance of purity evaluation and the potential of quantitative ^{1}H NMR as a purity assay. *J. Med. Chem.* **2014**, *57*, 9220-9231.

Graphical abstract